JAEA-Research
2009-030

JAEA-Research

Benchmark Calculation of APOLLO2 and SLAROM-UF in a Fast Reactor Lattice

Taira HAZAMA

Division of Nuclear Data and Reactor Engineering
Nuclear Science and Engineering Directorate

October 2009

Japan Atomic Energy Agency

日本原子力研究開発機構

本レポートは独立行政法人日本原子力研究開発機構が不定期に発行する成果報告書です。
本レポートの入手並びに著作権利用に関するお問い合わせは、下記あてにお問い合わせ下さい。
なお、本レポートの全文は日本原子力研究開発機構ホームページ（http://www.jaea.go.jp）
より発信されています。

独立行政法人日本原子力研究開発機構　研究技術情報部　研究技術情報課
〒319-1195　茨城県那珂郡東海村白方白根 2 番地 4
電話 029-282-6387, Fax 029-282-5920, E-mail:ird-support@jaea.go.jp

This report is issued irregularly by Japan Atomic Energy Agency
Inquiries about availability and/or copyright of this report should be addressed to
Intellectual Resources Section, Intellectual Resources Department,
Japan Atomic Energy Agency
2-4 Shirakata Shirane, Tokai-mura, Naka-gun, Ibaraki-ken 319-1195 Japan
Tel +81-29-282-6387, Fax +81-29-282-5920, E-mail:ird-support@jaea.go.jp

JAEA-Research 2009-030

Benchmark Calculation of APOLLO2 and SLAROM-UF in a Fast Reactor Lattice

Taira HAZAMA

Division of Nuclear Data and Reactor Engineering
Nuclear Science and Engineering Directorate
Japan Atomic Energy Agency
Tokai-mura, Naka-gun, Ibaraki-ken

(Received August 25, 2009)

A lattice cell benchmark calculation is carried out for APOLLO2 and SLAROM-UF on the infinite lattice of a simple pin cell featuring a fast reactor. The accuracy in k-infinity and reaction rates is investigated in their reference and standard level calculations.

In the 1st reference level calculation, APOLLO2 and SLAROM-UF agree with the reference value of k-infinity obtained by a continuous energy Monte Carlo calculation within 50 pcm. However, larger errors are observed in a particular reaction rate and energy range. A major problem common to both codes is in the cross section library of ^{239}Pu in the unresolved energy range.

In the 2nd reference level calculation, which is based on the ECCO 1968 group structure, both results of k-infinity agree with the reference value within 100 pcm. The resonance overlap effect is observed by several percents in cross sections of heavy nuclides.

In the standard level calculation based on the APOLLO2 library creation methodology, a discrepancy appears by more than 300 pcm. A restriction is revealed in APOLLO2. Its standard cross section library does not have a sufficiently small background cross section to evaluate the self-shielding effect of ^{56}Fe cross sections. The restriction can be removed by introducing the mixture self-shielding treatment recently introduced to APOLLO2.

SLAROM-UF original standard level calculation based on the JFS-3 library creation methodology is the best among the standard level calculations. Improvement from the SLAROM-UF standard level calculation is achieved mainly by use of a proper weight function for light or intermediate nuclides.

Keywords: SLAROM-UF, APOLLO2, Fast Reactor, Cell Calculation, Self-Shielding

格子計算コードAPOLLO2とSLAROM-UFの高速炉体系における比較

日本原子力研究開発機構
原子力基礎工学研究部門 核工学・炉工学ユニット
羽様　平

(2009年8月25日受理)

格子計算コードAPOLLO2とSLAROM-UFの無限増倍率と反応率の計算精度を高速炉燃料の無限ピンセル体系を対象に計算の詳細度毎に比較した。

参照解レベルの計算では、両コードによる無限増倍率計算結果は、連続エネルギーモンテカルロ計算による参照値と50pcm以内で一致した。しかしながら、反応率については反応の種類やエネルギー範囲によって有意な誤差が現れる。両コードに共通する問題点としては^{239}Puの非分離共鳴領域での誤差が挙げられる。

2番目の参照解レベルの計算として欧州の解析システムで使用されているECCO1968群に基づく計算を両コードで行い、無限増倍率が参照値と100pcm以内で一致することを確認した。1番目の参照解レベルに比べて群構造が粗いため共鳴干渉効果の評価精度が悪化し、重核種の断面積に数%の誤差が生じる。

標準レベルの計算では、各コード標準のライブラリを用いた場合に加え、ライブラリの作成方法をAPOLLO2の手法に統一した場合も評価した。同一手法のライブラリを用いた場合、無限増倍率の参照値からの差異が両コードともに300pcm以上の誤差が現れた。

APOLLO2の標準手法にはライブラリデータ及び計算手法の制限により^{56}Feの自己遮へい因子を適切に評価できないことが判明した。その制限は近年開発されたMixture処理を適用すれば解決できることを確認した。

SLAROM-UFの標準ライブラリを使用した場合は、標準レベルの計算の中では最も精度がよい。精度の向上は主にライブラリ作成時に適切な重み関数を使用することによる。

原子力科学研究所（駐在）：〒319-1195 茨城県那珂郡東海村白方白根2-4

Contents

目 次

List of Tables

List of Figures

This is a blank page.

1. Introduction

A lattice cell benchmark calculation is performed for cell calculation codes APOLLO2 and SLAROM-UF in the framework of the collaboration STC.4.2.1 between Commissariat à l'Energie Atomique (CEA) and Japan Atomic Energy Agency (JAEA). The accuracy in k-infinity and reaction rates are investigated in their reference and standard level calculations.

A comparison is made on the infinite lattice of a simple pin cell featuring a fast reactor, in which a difference mainly appears in the self-shielding treatment.

A larger error would be expected in APOLLO2 since it is optimized to thermal reactor analyses, especially in terms of the cross section library. Thus a special attention is paid on the library creation methodologies.

2. Calculation Codes

Outline of the calculation codes and calculation schemes employed in this work are described.

2.1 APOLLO2

APOLLO2[1)] is a modular multigroup transport code developed by CEA. The self-shielding effect is treated by a background cross section method or a sub-group method. The former method is used for resolved resonances in a standard level calculation. The latter is used in a reference level calculation and for unresolved resonances in the calculation of any level. The evaluated self-shielded (or effective) cross sections are then used to calculate flux distribution in a cell. A variety of flux solvers are available.

2.1.1 Background cross section method

A method with the background cross section is employed in the resolved resonance range in the standard level calculation.

2.1.1.1 Creation of cross section library

For a mixture of a resonant isotope and moderator (non-resonant) isotopes, the neutron slowing down equation in the absence of fission source is given by

$$\left[N_0\sigma_{0,t}(u)+\sum_m N_m\sigma_{m,t}(u)\right]\Phi(u)=N_0 r_0\Phi(u)+\sum_m N_m r_m\Phi(u), \tag{2.1.1}$$

where u is the lethargy, Φ is the flux, σ_x is the microscopic cross section for reaction x (t=total, s=elastic scattering), N is the density, and r is slowing down operator. The subscript "0" and "m" denote that the values are on the resonant and moderator isotopes, respectively.

An assumption is introduced that the slowing down terms can be described by the isotropic elastic scattering in the center of mass system:

$$\begin{aligned} r\Phi(u) &= \int_{u-\varepsilon}^{u}\sigma_s(u')\,p(u'\to u)\Phi(u')\,du' \\ p(u'\to u) &= \frac{exp(u'-u)}{1-\alpha}, \end{aligned} \tag{2.1.2}$$

where $\alpha=\left(\frac{A-1}{A+1}\right)^2$ (A: the atomic mass) and ε is the maximum lethargy gain ($\varepsilon=-\ln\alpha$).

In addition, following assumptions are made:

- Moderator isotopes are pure scattering materials, that is, $\sigma_{m,t}=\sigma_{m,s}$.
- $\sigma_{m,x}(u)$ is constant ($=\sigma^g_{m,x}$) for $u\in g$.
- The slowing down term by the moderator, $r_m\Phi$, is expressed by a product of smooth function $C(u)$ and total (=scattering) cross section $\sigma_{m,t}$.

Then we obtain

$$\Phi(u)\approx\frac{r_0\Phi(u)+\sigma_b^g C(u)}{\sigma_{0,t}(u)+\sigma_b^g}, \tag{2.1.3}$$

where σ_b^g is the background cross section for the resonant isotope and group g, $\sigma_b^g=\frac{1}{N_0}\sum_m N_m\sigma^g_{m,t}$.

Using Eq. (2.1.3), Φ is calculated and the lethargy integrated reaction rate for resonant isotope 0, reaction x, and group g, $T^{hom,g}_{0,x}(=\int_{u\in g}\sigma_{0,x}(u)\Phi(u)du)$, is obtained.

This calculation is carried out with NJOY[2)] (using the flux calculator option of GROUPR module). The smooth function $C(u)$ is set to 1 (1/E weight). The evaluated reaction rates are stored in the cross section library as a function of the background cross section and temperature T (resonant cross section depending on T).

2.1.1.2 Livolant-Jeanpierre approach

The effective cross section is calculated based on a double equivalence step: (a) a homogenization step and (b) a multigroup equivalence step.

In the homogenization step, an equivalent background cross section is evaluated for a resonant isotope so that the microscopic absorption reaction rate of the isotope in a heterogeneous region is reproduced in the corresponding (having the same composition of the resonant isotope) homogeneous system.

In the multigroup equivalence step, the microscopic effective cross section is evaluated so that the reaction rate obtained in the homogenization step is reproduced by a set of the effective cross section and the flux solved in a multigroup slowing down equation.

(1) Homogenization step

Reaction rates are calculated in a heterogeneous and homogeneous systems under the common approximations:

- $\sigma_{m,x}(u)$ is constant $(= \sigma^g_{m,x})$ for $u \in g$.
- The slowing term by the resonant isotope is written as $r_0\Phi(u) \approx \psi r_0\varphi(u)$, where ψ and φ are global and local components of $\Phi(= \psi\varphi)$.
- Global flux ψ is independent of regions.
- The slowing term by the resonant isotope is expressed by the TR (Total Resonance) approximation.

(a) sub-step 1 (heterogeneous calculation)

The absorption reaction rate is calculated in a heterogeneous system.

In a heterogeneous system, the slowing down equation for a mixture of a resonant isotope and moderator isotopes is given by

$$V_i\Sigma_{i,t}(u)\Phi_i(u) = \sum_j \left[P_{j\to i}(u)\, V_j \left\{ N_{0,j} r_{0,j}\Phi_j(u) + \sum_m N_{m,j} r_{m,j}\Phi_j(u) \right\} \right], \tag{2.1.4}$$

where V is the volume, Σ_x is the macroscopic cross section for reaction x, and $P_{j\to i}$ is the probability for a neutron born in region j to have its first collision in region i. The subscript "i" and "j" denote that the values are on the corresponding regions.

Applying the first three of the common approximations, we obtain

$$\varphi_i(u) = \sum_j [C_{i,j}(u) r_{0,j}\varphi_j(u)] + S_i(u), \tag{2.1.5}$$

where

$$\begin{aligned} C_{i,j}(u) &= \frac{P_{j\to i}(u)\, V_j N_{0,j}}{V_i\Sigma_{i,t}(u)} \\ S_i(u) &= \frac{\sum_j \left[P_{j\to i}(u)\, V_j \Sigma^g_{m,j,s} \right]}{V_i\Sigma_{i,t}(u)}. \end{aligned}$$

When the TR approximation is applied, the term, $r_{0,j}\varphi_j$, is expressed by

$$r_{0,j}\varphi_j(u) \approx \sum_{g' \le g} \left[prop(g' \to g) \left\langle \sigma_{0,j,s}(u')\varphi_j(u') \right\rangle^{g'} \right], \tag{2.1.6}$$

where $prop(g' \to g)$ is related to the probability that a neutron scatters from group g' into group g. Here, the following assumptions are used:

- Lethargy gain by scattering is so small that the term $exp(u' - u)$ in Eq. (2.1.2) is replaced by a constant with the condition $\int_{u-\varepsilon_0}^{u} p(u' \to u)du' = 1$, that is, $(1 - \alpha_0)/\varepsilon_0$, then

$$r_0\varphi(u) \approx \frac{1}{\varepsilon_0} \int_{u-\varepsilon_0}^{u} \sigma_{0,s}(u')\,\varphi(u')\,du'. \tag{2.1.7}$$

- For lethargy u' belonging to energy group g', the product $\sigma_{0,s}(u')\,\varphi_j(u')$ is described by the average value $\left\langle \sigma_{0,s}(u')\varphi_j(u') \right\rangle^{g'}$.

The values of $prop(g' \to g)$ is a function of ε_0 and calculated in APOLLO2.

Then the scattering reaction rate based on the TR approximation for region i and the resonant isotope is given by

$$\begin{aligned} T_{0,i,s}^{TR,het,g} &= \sum_j \left[K_j^g + prop(g \to g) \frac{1}{\Delta u^g} T_{0,i,s}^{TR,het,g} \right] \int_{u \in g} \sigma_{0,s}(u) C_{i,j}(u) du & (2.1.8) \\ &\quad + \int_{u \in g} \sigma_{0,s}(u) S_i(u) du & (2.1.9) \\ K_j^g &= \sum_{g' < g} \left[prop(g' \to g) \frac{1}{\Delta u^{g'}} T_{0,j,s}^{TR,het,g'} \right]. \end{aligned}$$

The integrals in the equation are calculated by a quadrature formula with the probability table (as in a sub-group method) and $T_{0,i,s}^{TR,het,g}$ can be solved in the ascending group order. Once $T_{0,i,s}^{TR,het,g}$ is obtained, the absorption reaction rate $T_{0,i,a}^{TR,het,g}$ is calculated in a similar manner.

(b) sub-step 2 (homogeneous calculation)

The absorption reaction rate is calculated in the homogeneous system containing the resonant isotope with the same composition as in the heterogeneous region of interest.

In a homogeneous system, under the common approximations, Eq. (2.1.1) reduces to

$$\left[\sigma_{0,t}(u) + \sigma_{eb}^g \right] \varphi(u) = \sum_{g' \le g} \left[prop(g' \to g) \left\langle \sigma_{0,s}(u)\varphi(u) \right\rangle^{g'} \right] + \gamma_b^g \sigma_{eb}^g, \tag{2.1.10}$$

where γ_b^g is the effective ratio of the macroscopic scattering cross section of moderator to the total for resonant isotope 0 in the region i, and σ_{eb}^g is the equivalent background cross section defined by

$$\sigma_{eb}^g = \frac{1}{\sum_j C_{i,j}(u)} - \sigma_{0,t}(u) \text{ (assumed constant in group g).} \tag{2.1.11}$$

γ_b^g is obtained by

$$\gamma_b^g = \int_{u \in g} \frac{S_i(u)}{1 - \sigma_{0,t}(u) \sum_j C_{i,j}(u)} du, \tag{2.1.12}$$

assuming that $r_{0,j}\varphi_j(u)$ of Eq. (2.1.5) is independent of region j. It is calculated in the sub-step 1 using a quadrature formula.

The scattering reaction rate, $T_{0,s}^{TR,hom,g}$, is then written as

$$T_{0,s}^{TR,hom,g} = \left[K^g + prop(g \to g) \frac{1}{\Delta u^g} T_{0,s}^{TR,hom,g} + \gamma_b^g \sigma_{eb}^g \right] I^g, \tag{2.1.13}$$

where

$$K^g = \sum_{g'<g} \left[prop(g' \to g) \frac{1}{\Delta u^{g'}} T_{0,s}^{TR,hom,g'} \right]$$
$$I^g = \frac{1}{\Delta u^g} \int_{u \in g} \frac{\sigma_{0,s}(u)}{\sigma_{0,t}(u) + \sigma_{eb}^g} du.$$

The integral I^g is calculated by a quadrature formula with the probability table, and $T_{0,s}^{TR,hom,g}$ can be solved in the ascending group order for a given σ_{eb}^g and the calculated γ_b^g. Once $T_{0,s}^{TR,hom,g}$ is obtained, the absorption reaction rate, $T_{0,a}^{TR,hom,g}$, is calculated in a similar manner.

(c) sub-step 3 (equivalent background cross section)

The equivalent background cross section σ_{eb}^g is searched in the homogeneous system so that the absorption reaction rate in the homogeneous system becomes equal to that in the heterogeneous system:

$$T_{0,a}^{TR,hom,g}(\sigma_{eb}^g) = T_{0,a,i}^{TR,het,g}. \tag{2.1.14}$$

Then σ_{eb}^g is used as the background cross section σ_b^g to obtain $T_{0,x,\mathrm{lib}}^{hom,g}$, the reaction rate based on the cross section library as

$$T_{0,i,x}^{het,g} = \gamma_b^g T_{0,x,\mathrm{lib}}^{hom,g}(\sigma_b^g = \sigma_{eb}^g). \tag{2.1.15}$$

This procedure is justified since Eq. (2.1.10) is similar to Eq. (2.1.3) and is linear on γ_b^g.

In this way, the precise slowing down treatment based on the flux calculator in NJOY is reflected.

These homogenization steps are repeated for each region and each resonant isotope included in a system to be solved.

(d) sub-step 4 (transfer matrix self-shielding, TRSS option)

This step is not included in the standard version of APOLLO2 and specially introduced to avoid a problem encountered in a fast reactor analysis (see Appendix A).

In the step, the effective scattering transfer matrix $\sigma_{0,i,s}^{het,g' \to g}$ is evaluated using a self-shielding factor table additionally prepared in the library creation process.

Then the probability that a neutron scatters from group g' into group g is evaluated by

$$p_{0,i}^{g' \to g} = \frac{\sigma_{0,i,s}^{het,g' \to g}(\sigma_{b,i}^g)}{\sum_g \sigma_{0,i,s}^{het,g' \to g}(\sigma_{b,i}^g)} \tag{2.1.16}$$

(2) multigroup equivalence step

A set of the effective cross section $\sigma_{0,x,i}^g$ and the flux φ_i^g is iteratively calculated preserving the reaction rate obtained in the homogenization step, that is,

$$\sigma_{0,x,i}^g = \frac{T_{0,i,x}^{het,g}(\sigma_{b,i}^g)}{\Delta u^g \varphi_i^g} \tag{2.1.17}$$

The flux φ_i^g is given by a multigroup form of Eq. (2.1.5):

$$\varphi_i^g = \frac{1}{\Delta u^g} \sum_j \left[\sum_{g' \le g} \left[p_0^{g' \to g} T_{0,i,s}^{het,g'}(\sigma_{b,j}^{g'}) \right] C_{i,j}^g \right] + S_i^g \tag{2.1.18}$$

,where

$$C_{i,j}^{g} = \frac{P_{j\to i}^{g} V_j N_{0,j}}{V_i \Sigma_{i,t}^{g}} \tag{2.1.19}$$

$$S_{i}^{g} = \frac{\sum_{j} \left[P_{j\to i}^{g} V_j \Sigma_{m,j} \right]}{V_i \Sigma_{i,t}^{g}}. \tag{2.1.20}$$

$P_{j\to i}^{g}$ is a function of the macroscopic effective total cross sections.

$p_0^{g'\to g}$ is the probability that a neutron scatters from group g' into group g, and is calculated in the sub-step 4 (TRSS option). (in the standard APOLLO2, infinite dilution scattering reaction is used.)

The equation is solved by iteration keeping $T_{0,i,s}^{het,g}(\sigma_{b,i}^{g})$. In the first iteration, the flux φ_i^g is set to unity, then $\Sigma_{i,t}^{g}$ is obtained by Eqs. (2.1.17) and (2.1.21), and the flux is updated by Eq. (2.1.18).

$$\Sigma_{i,t}^{g} = N_{0,i}\sigma_{0,t,i}^{g} + \Sigma_{m,i,t}^{g}. \tag{2.1.21}$$

2.1.2 Sub-group method

A sub-group method is employed in the reference level calculation and in the unresolved resonance range of the standard level calculation.

For a mixture of a resonant isotope and moderator (non-resonant) isotopes, the neutron slowing down equation is given by

$$V_i \Sigma_{i,t}(u)\Phi_i(u) = \sum_j \left[P_{j\to i}(u)\, V_j \tau_j(u)\right] \tag{2.1.22}$$

$$\tau_j(u) = R_{0,j}\Phi_j(u) + R_{m,j}\Phi_j(u) + Q_j(u),$$

where τ is a source term, $R = Nr$, and Q is an external source.

Then lethargy averaged flux and reaction rate are written as

$$\langle \Phi_i(u)\rangle^g = \sum_j \frac{V_j}{V_i} \left\langle \frac{P_{j\to i}(u)}{\Sigma_{i,t}(u)} \tau_j(u) \right\rangle^g \tag{2.1.23}$$

$$\langle \sigma_x(u)\Phi_i(u)\rangle^g = \sum_j \frac{V_j}{V_i} \left\langle \sigma_x(u) \frac{P_{j\to i}(u)}{\Sigma_{i,t}(u)} \tau_j(u) \right\rangle^g . \tag{2.1.24}$$

Here we introduce an approximation:

- cross section σ_x is not correlated to the source term τ.

Then the equations can be written as

$$\langle \Phi_i(u)\rangle^g = \sum_j \frac{V_j}{V_i} \left\langle \frac{P_{j\to i}(u)}{\Sigma_{i,t}(u)} \right\rangle^g \langle \tau_j(u)\rangle^g \tag{2.1.25}$$

$$\langle \sigma_x(u)\Phi_i(u)\rangle^g = \sum_j \frac{V_j}{V_i} \left\langle \sigma_x(u) \frac{P_{j\to i}(u)}{\Sigma_{i,t}(u)} \right\rangle^g \langle \tau_j(u)\rangle^g . \tag{2.1.26}$$

The coefficients $\left\langle \frac{P_{j\to i}(u)}{\Sigma_{i,t}(u)} \right\rangle^g$ and $\left\langle \sigma_x(u) \frac{P_{j\to i}(u)}{\Sigma_{i,t}(u)} \right\rangle^g$ are calculated by a quadrature formula with the probability table created by CALENDF[3] code.

The slowing terms are written as

$$\frac{1}{\Delta u^g} \int_{u\in g} R_{0,j}\Phi_j(u)du = \frac{1}{\Delta u^g} \sum_{g'\le g} p_{0,j}^{g'\to g} \Delta u^{g'} \left\langle \Sigma_{0,j,s}(u')\, \Phi_j(u') \right\rangle^{g'} \tag{2.1.27}$$

$$\frac{1}{\Delta u^g} \int_{u\in g} R_{m,j}\Phi_j(u)du = \frac{1}{\Delta u^g} \sum_{g'\le g} p_{m,j}^{g'\to g} \Delta u^{g'} \left\langle \Sigma_{m,j,s}(u')\, \Phi_j(u') \right\rangle^{g'} \tag{2.1.28}$$

Unlike in the previous section, the probability, $p_{0,j}^{g'\to g}$ is approximately calculated by the infinite dilution cross section, since the self-shielding effect on the probability is not large in the fine energy group structure.

The second term is more simply written as

$$\frac{1}{\Delta u^g} \int_{u\in g} R_{m,j}\Phi_j(u)du \quad = \quad \frac{1}{\Delta u^g} \sum_{g'\le g} p_{m,j}^{g'\to g} \Sigma_{m,j,s}^{g'} \Delta u^{g'} \left\langle \Phi_j(u') \right\rangle^{g'} . \tag{2.1.29}$$

Then the source term is obtained by

$$\langle \tau_j(u)\rangle^g = \frac{1}{\Delta u^g} \sum_{g'\le g} p_{0,j}^{g'\to g} \Delta u^{g'} \left\langle \Sigma_{0,j,s}(u')\, \Phi_j(u') \right\rangle^{g'} + \frac{1}{\Delta u^g} \sum_{g'\le g} p_{m,j}^{g'\to g} \Sigma_{m,j,s}^{g'} \Delta u^{g'} \left\langle \Phi_j(u') \right\rangle^{g'} + \langle Q_j(u)\rangle^g . \tag{2.1.30}$$

This equation is solved in the ascending group order using Eqs. (2.1.23) and (2.1.24). Then the effective microscopic cross section is obtained from Eqs. (2.1.25) and (2.1.26).

2.2 SLAROM-UF

SLAROM-UF[4] is a lattice cell calculation code for fast reactor analyses developed by JAEA. Its reference level calculation is based on a combination of a fine group calculation (max. 900 groups) and an ultra-fine group (UF) calculation (approx. 100000 groups). In a normal calculation procedure, the fine group calculation is first carried out to obtain effective cross sections based on a background cross section method. In case of a heterogeneous cell, Tone method is employed to evaluate the background cross section. Then the UF calculation is carried out to replace effective cross sections over the energy range below about 50 keV. Thus obtained cross sections are then used to calculate flux distribution by the collision probability method for a heterogeneous cell or by solving the B1 equation for a homogeneous cell. The standard level calculation uses a coarse group cross section library without the UF calculation process.

2.2.1 Background cross section method

A method with the background cross section is employed in the standard level calculation and over the energy range higher than about 50 keV in the reference level calculation.

2.2.1.1 Creation of cross section library

The creation procedure of the library is similar to that in APOLLO2. The library is created mainly by NJOY and self-shielding data are tabulated as a function of the background cross section and temperature.

Major differences from APOLLO2 are as follows:

- Effective cross sections are tabulated in stead of reaction rates.
- The elastic removal cross section is stored for self-shielding treatment of the scattering transfer matrix.
- The narrow resonance (NR) approximation is used.
- NJOY process starts with the pointwise evaluated nuclear data file (PENDF) created with PREPRO2004[6] (LINEAR, RECENT, and SIGMA1).

The NR approximation is used because of two reasons: (a) A special care was paid in the standard level calculation as described later. (b) In the reference calculation, group structure is so fine above 50 keV that the approximation is valid and accuracy below 50 keV is assured by the UF calculation.

The default library set contains libraries of three different group structures. One is a JFS-type[5] 70 group library for the standard level calculation. The others are 175 and 900 group libraries for the reference level calculation.

The 175 and 900 group libraries are created by NJOY with a standard weight function of Maxwellian + 1/E + fission spectrum. On the contrary, the 70 group library is created with a special weight function. In addition, data for major heavy nuclides are created by TIMS[7]. More details of the 70 group library are described below.

(1) Library based on NJOY

Under the NR approximation, the flux is written as

$$\Phi(u) \propto \frac{C(u)}{\sigma_{0,t}(u) + \sigma_b^g}. \tag{2.2.1}$$

In the 70 group library, a collision density calculated for a typical fuel assembly of the Japanese sodium-cooled fast reactor "Monju" is used. It is calculated using a very fine group homogeneous cell calculation ($\sim$ 5,000 groups), that is,

$$C(u) = \frac{\Sigma_{M,t}^{fg}\Phi_M^{fg}}{\Delta u^{fg}} \text{ for } u \in fg, \tag{2.2.2}$$

where "fg" means a group in the very fine group calculation and M" denotes the value is on "Monju".

Then the flux is written as

$$\Phi(u) \propto \frac{\Sigma_{M,t}^{fg}\Phi_M^{fg}}{\sigma_{0,t}(u) + \sigma_b^{fg}} \text{ for } u \in fg. \tag{2.2.3}$$

Dividing $\Sigma_{M,t}$ by the atomic density of a resonant material and expressing it by the resonance term $\sigma_{0,t}$ and the background cross section term $\sigma_{M,b}^{fg}$, we obtain

$$\Phi(u) \propto \frac{\left(\sigma_{0,t}^{fg} + \sigma_{M,b}^{fg}\right)\Phi_M^{fg}}{\sigma_{0,t}(u) + \sigma_b^{fg}} \text{ for } u \in fg. \tag{2.2.4}$$

Use of the collision density serves to make Φ closer to Φ_M^{fg} by reducing the variation in $\sigma_{0,t}$, so that broad group cross sections averaged with Φ_M^{fg} would be reconstructed having the background cross section as a variable. If the condition,

$$\frac{\sigma_{0,t}^{fg} + \sigma_{M,b}^{fg}}{\sigma_{0,t}(u) + \sigma_b^{fg}} \approx const. \tag{2.2.5}$$

is satisfied, the broad group cross sections becomes that of the "Monju" core.

(2) Library based on TIMS

TIMS solves the slowing down equation by an ultra-fine group calculation. Two resonant isotopes and a fictitious moderator can be considered as

$$\Sigma_t(u)\Phi(u) = N_{0,1}r_{0,1}\Phi(u) + N_{0,2}r_{0,2}\Phi(u) + \sum_m N_m r_m \Phi(u), \tag{2.2.6}$$

where the subscripts "1" and "2" denote the 1st and the 2nd resonant isotopes.

Using the assumptions:

- Moderator isotopes are pure scattering materials with isotropic elastic scattering in the center of mass system.
- $\sigma_{m,x}(u)$ is constant $(= \sigma_{m,x}^g)$ for $u \in g$.

and using the definition of the background cross section, we obtain

$$\sigma_t(u)\Phi(u) = r_{0,1}\Phi(u) + R_2 r_{0,2}\Phi(u) + \sigma_b^g \int_{u-\varepsilon_m}^{u} \frac{exp(u'-u)}{1-\alpha_m}\Phi(u')du', \tag{2.2.7}$$

where R_2, called R-factor, is the density ratio of the 2nd resonant isotope to the 1st. α_m is determined so that it can represents all moderator isotopes in a system. The fictitious atomic mass, $A = 30$, is used as default.

The flux is calculated by solving Eq. (2.2.7) with an ultra fine group using the recurrence formula developed by Kier[8].

Then self-shielding factors are calculated and stored in the cross section library as a function of the background cross section, temperature, and R-factor. In the present 70 group library, TIMS is used for three combinations of the 1st and the 2nd resonant isotope; (^{238}U, ^{239}Pu), (^{238}U, ^{235}U), and (^{239}Pu, ^{238}U).

This tabulation is applied to the unresolved resonance range as well. In the case, a fictitious ladder of resonance cross sections are generated in TIMS by a Monte Carlo method keeping the average values of unresolved resonance parameters within assumed errors (of several percents).

2.2.1.2 Tone method

Tone method[9] is used to evaluate the background cross section in a heterogeneous cell.
Starting from Eq. (2.1.22);

$$V_i \Sigma_{i,t}(u) \Phi_i(u) = \sum_j \left[P_{j \to i}(u)\, V_j \tau_j(u) \right], \tag{2.2.8}$$

we introduce an approximation:

$$\frac{P_{j \to i}(u)}{\Sigma_{i,t}(u)} \approx f_i(u) \frac{P^g_{j \to i}}{\Sigma^g_{i,t}}. \tag{2.2.9}$$

It is based on the assumption that the ratio varies slowly with lethargy and does not depend on the region j, considering $P_{j \to i}(u)$ is a function of $\Sigma_{i,t}(u)$.
Using the reciprocity relation

$$V_i P_{i \to j}(u)\, \Sigma_{i,t}(u) = V_j P_{j \to i}(u)\, \Sigma_{j,t}(u), \tag{2.2.10}$$

Eq. (2.2.9) can be written as

$$P^g_{j \to i} V_j \Sigma_{j,t}(u) f_i(u) \quad = \quad V_i P_{i \to j}(u)\, \Sigma^g_{i,t}. \tag{2.2.11}$$

Taking summation over regions and using the normalization condition, $\sum_j P_{i \to j}(u) = 1$, we obtain

$$f_i(u) \quad = \quad \frac{V_i \Sigma^g_{i,t}}{\sum_j P^g_{j \to i} V_j \Sigma_{j,t}(u)}. \tag{2.2.12}$$

Substituting Eq. (2.2.9) to Eq. (2.2.8), and assuming the source term τ is constant within a group, we obtain

$$\Phi_i(u) \quad = \quad f_i(u) \sum_j \left[\frac{V_j P^g_{j \to i}}{V_i \Sigma^g_{i,t}} \tau^g_j \right]. \tag{2.2.13}$$

In this expression, the lethargy dependence of the flux is determined by f_i, then

$$\Phi_i(u) \quad \propto \quad \frac{1}{\sum_j P^g_{j \to i} V_j \Sigma_{j,t}(u)}. \tag{2.2.14}$$

Expressing $\Sigma_{j,t}$ by a resonant and the moderator terms:

$$\Sigma_{j,t}(u) = N_{0,j} \sigma_{0,t}(u) + \Sigma^g_{m,j,t}, \tag{2.2.15}$$

we obtain the relation:

$$\Phi_i(u) \quad \propto \quad \frac{1}{\sigma_{0,t}(u) + \sigma^g_{Tone,b,i}}, \tag{2.2.16}$$

where

$$\sigma^g_{Tone,b,i} \quad = \quad \frac{\sum_j P^g_{j \to i} V_j \Sigma^g_{m,j,t}}{\sum_j P^g_{j \to i} V_j N_{0,j}}. \tag{2.2.17}$$

Eq. (2.2.16) has the same lethargy dependence as Eq. (2.2.1) with $C(u) = const.$, indicating that the equivalent background cross section that relates a heterogeneous cell to the homogeneous cell can be defined by Eq (2.2.17).
Then the effective cross sections (including scattering transfer matrix) are obtained by interpolating $\sigma^g_{b,i}$ in the background cross sections.

2.2.2 UF calculation method

The UF calculation method is employed over the energy range below about 50 keV in the reference level calculation. The calculation is carried out after the calculation of effective cross sections by the background cross section method.

The methodology is the same as that in TIMS. It solves the slowing down equation in an ultra-fine group structure using the recurrence formula developed by Kier, and uses a fictitious ladder of cross sections for unresolved resonances.

The differences are in the capability to handle a heterogeneous system and any number of isotopes. The flux is calculated by the following slowing down equation:

$$\sigma_{t,i}(u)\Phi_i(u) = \sum_j P_{j\to i}(u)V_j \sum_k \int_{u-\varepsilon_k}^{u} N_k\sigma_{k,s}(u')\frac{exp(u'-u)}{1-\alpha_k}\Phi_j(u')du'. \quad (2.2.18)$$

SLAROM-UF uses the PENDF data created in PREPRO2004 and TIMS; from which about 100000 group cross section data are created in SLAROM-UF for a user-specified temperature.

Thus calculated neutron flux in the ultra-fine group structure is used to obtain effective cross sections in the group structure specified in the previous step. Then cross sections in the previous step are replaced on capture, fission, elastic scattering, and elastic removal reactions. Improvements are achieved on the self-shielding effects as well as on the infinite dilution cross sections by reflecting the precise neutron spectrum of the calculated system.

2.3 Calculation Schemes

Two levels of calculation schemes, standard and reference level calculations, are tested in each code as listed below. In the standard calculation scheme of SLAROM-UF, a library equivalent to APOLLO2 is prepared to remove an influence of the library creation methodology.

AP11276 APOLLO2 reference level calculation (11276 groups) with the sub-group method

AP172 APOLLO2 standard level calculation (XMAS 172 groups) with the sub-group method for unresolved resonances and with the background cross section method for resolved resonances.

UF900 SLAROM-UF reference level calculation (combination of 900 fine group calculation and the UF calculation)

SLA172 SLAROM-UF standard level calculation (XMAS 172 groups without the UF calculation). A 172 group library was created reflecting the energy group structure and methodology employed in creation of the APOLLO2 172 group library.

SLA172JFS SLAROM-UF original standard level calculation (XMAS 172 groups without the UF calculation). This is an equivalence of the 70 group standard calculation scheme of SLAROM-UF. A 172 group library was created using the methodology employed in the SLAROM-UF 70 group library.

In addition, the 2nd reference level calculation are tested, where ECCO 1968 group structure [10] is employed.

AP1968 APOLLO2 2nd reference level calculation with the sub-group method. This is equivalent to the reference level calculation employed in ECCO system dedicated to the fast reactor analyses in CEA.

SLA1968 SLAROM-UF 2nd reference level calculation without the UF calculation. A 1968 group library was created reflecting the methodology employed in creation of APOLLO2 172 group library.

Cross section libraries used in the above calculation schemes are briefly compared in Table 2.1. In this test, the evaluated nuclear data file JEFF3.1 [13] is used in all the calculations.

Table 2.1 Comparison of cross section libraries used in the calculations

	Calculation scheme				
	AP11276, AP1968	AP172	UF900, SLA1968	SLA172	SLA172 JFS
PENDF	NJOY (RECONR, THERMR, BROADR)		PREPRO2004(LINEAR, RECENT, SIGMA1), NJOY(BROADR)		
GENDF	NJOY(UNRESR, GROUPR(NR approx. with weight function of Maxwellian + 1/E + fission spectrum))	same as AP11276 except use of flux calculator with weight function of 1/E in GROUPR for resolved resonances	same as AP11276 except use of PURR[a)]	same as AP172[b)] except use of PURR	same as SLA1968 except for weight function [c)]
Dilution points	none	65 points originally created and later reduced considering interpolation error	9 points (0.1, 1, 10, 35, 100, 10^3, 10^4, 10^5, 10^6)		
Special library	probability table created with CALENDF (for the sub-group method)		PENDF prepared with PREPRO2004 + pseud PENDF created with TIMS for unresolved resonance (used in the ultra-fine group calculation[d)])	none	TIMS for ^{238}U and ^{239}Pu

a) PURR is used for better equivalence to the sub-group calculation of APOLLO2. In the SLAROM-UF original library, UNRESR is used.
b) Different weight function of Maxwellian+1/E+fission spectrum is used but effectively the same in the resonance energy range of interest.
c) Collision density calculated in "MONJU" fuel assembly is used.
d) Ultra-fine group cross sections (100,000g) at a user-specified temperature are constructed in SLAROM-UF.

Energy group structures in the above calculation schemes are shown in Fig.2.1 for energy range of interest in this work (see Fig. 3.1). In the 900 group structure, a coarser energy mesh structure is employed below about 50 keV where the self-shielding effect should be evaluated by the UF calculation. The group structure of the UF calculation is listed in Table 2.2.

Reference values are obtained with continuous energy Monte Carlo codes TRIPOLI4[11] (CEA) and MVP[12] (JAEA). Both codes use the probability table for unresolved resonances. In this report, results with MVP are used as a reference unless specified.

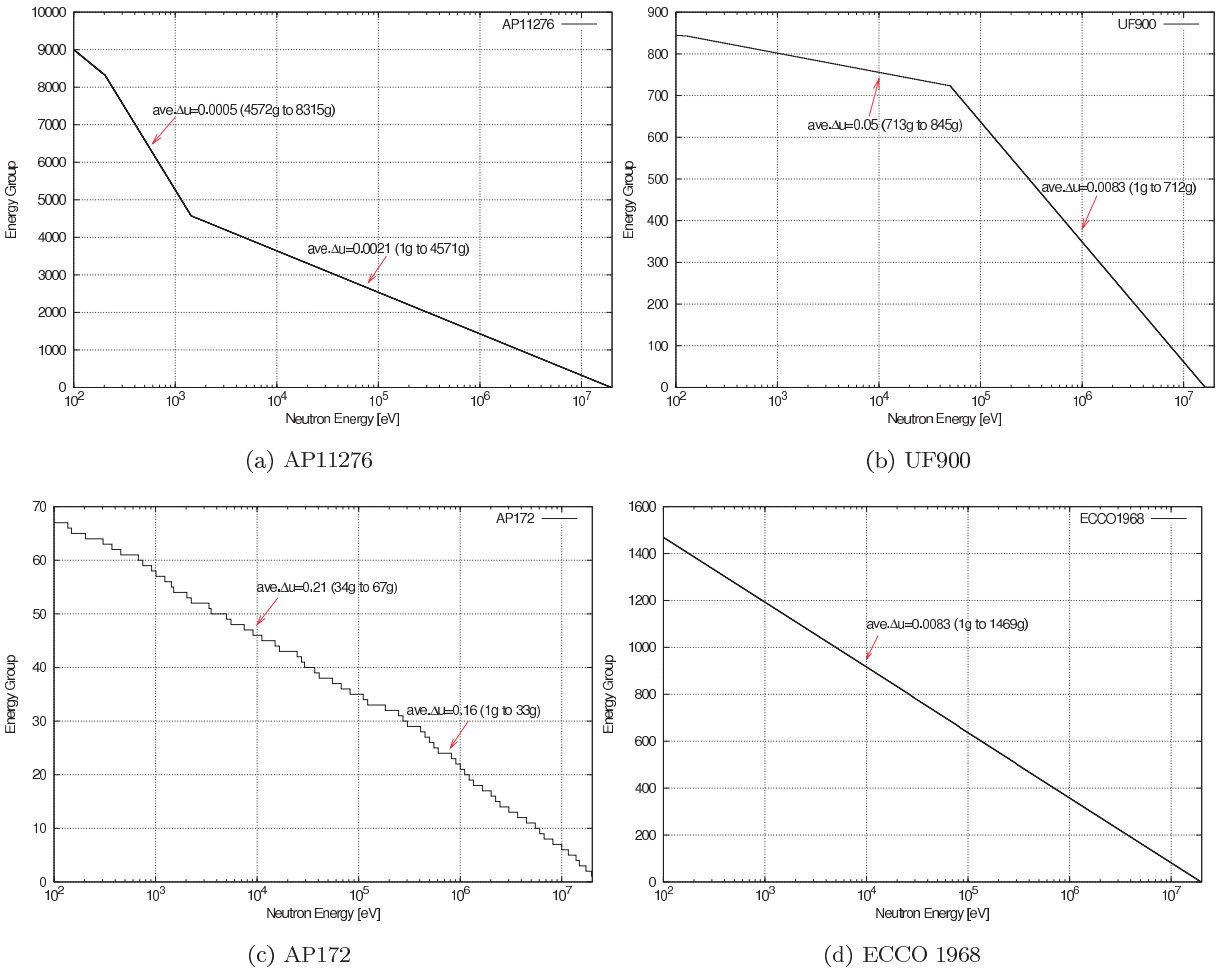

(a) AP11276 (b) UF900

(c) AP172 (d) ECCO 1968

Fig. 2.1 Energy group structures of employed calculation schemes

Table 2.2 Energy group structure of UF calculation

Energy range (eV)	Lethargy width ($\times 10^{-5}$)	Number of groups
52475-9118.8	3.125	56,000
9118.8-4307.4	6.250	12,000
4307.4-961.12	12.500	12,000
961.12-130.07	25.000	8,000
130.07-0.11861	50.000	14,000

3. Benchmark Data

A cylindrical fuel pin cell model was prepared featuring a fuel assembly of the French fast reactor "SuperPhenix". The cell is comprised of three regions; fuel, cladding, and coolant with homogenized wrapper tube. The fissile materials in the fuel region are represented by ^{239}Pu and the structural materials are by ^{56}Fe. The specifications of the cell are listed in Table 3.1.

Table 3.1 Material composition (barn·cm)

Region	Fuel	Cladding	Coolant	Homogeneous
^{238}U	2.20094E-02	-	-	8.78186E-03
^{239}Pu	3.48900E-03	-	-	1.39213E-03
^{240}Pu	1.14759E-03	-	-	4.57894E-04
^{16}O	5.32919E-02	-	-	2.12637E-02
^{56}Fe	-	8.47660E-02	2.01709E-02	2.28763E-02
^{23}Na	-	-	2.32498E-02	1.01024E-02
Radius(cm)	0.35700	0.42500	0.56517	-

Temperature is all set to 300K.

The cell-total neutron spectrum (flux per lethargy) and reaction rates are shown in Fig. 3.1. The flux is normalized in the volume and energy integrated value. The reaction rates are noticeable from 100 eV to 10 MeV.

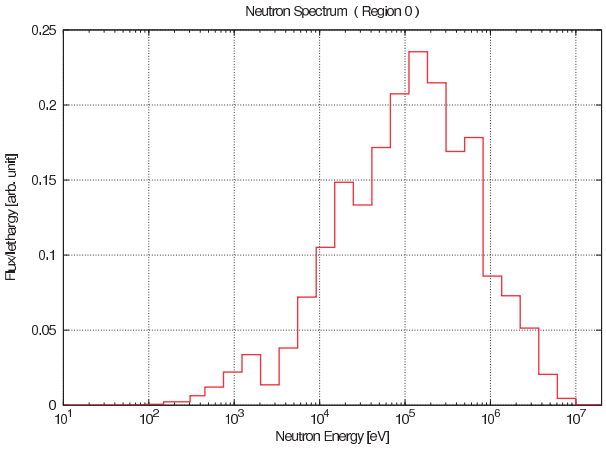

(a) Neutron Spectrum

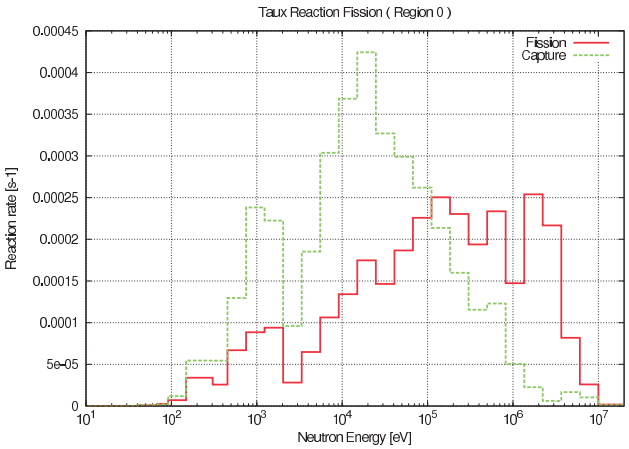

(b) Reaction rate

Fig. 3.1 Feature of the benchmark model (MVP)

4. Results

Results are summarized in this section for the heterogeneous model. The homogeneous model is referred only in a discussion. In the calculation, the iteration procedure on the background cross section, which is often used to take into account the resonance overlap effect among different nuclides, is not used to simplify the comparisons. Its influence will be discussed in Section 5.4.3.

The following parameters are compared between the codes and among the calculation schemes:

- k-infinity
- Reaction rate
- Neutron spectrum

The volume and energy integrated flux is normalized to unity in the evaluation of the reaction rate and neutron spectrum.

The results by MVP and TRIPOLI are all based on the track length estimator. The flux and reaction rates are tallied in ECCO 33 group structure[10] and their uncertainties are summed up by the root sum square if necessary. Cross sections are obtained by dividing the reaction rates by the flux.

The summary of k-infinity calculations is listed in Table 4.1. An energy break-down is shown for energy ranges higher and lower than 40.9 keV (upper boundary of 13th group in ECCO 33 structure), where the k-infinity is expressed by the macroscopic reaction rate ratio as:

$\mathrm{k-infinity} = \mathrm{Production\ term}/\mathrm{Absorption\ term}$,

$\mathrm{Production\ term} = \nu\Sigma_f\Phi$,

$\mathrm{Absorption\ term} = \Sigma_a\Phi - \Sigma_{n2n}\Phi - \Sigma_{n3n}\Phi$[*1].

In the reference level calculations (AP11276 and UF900), the results of the k-infinity agree to the reference within 50 pcm, while the standard level calculations (AP172 and SLA172) differ by more than 300 pcm. In the 2nd reference level calculations (AP1968 and SLA1968) and in the SLAROM-UF original standard calculation (SLA172JFS), the accuracies are nearly as good as those in the reference level calculations.

When compared on the energy break-down, differences in accuracy are not so clear. SLA172JFS and SLA1968 look best among all the calculation schemes.

Table 4.2 shows the comparison on the reaction rates. Unlike in the reaction rate ratio, the standard calculations show poor accuracy with about 1,000pcm of errors in the Etotal values. The other schemes have similar accuracy and SLA1968 is the best.

Table 4.3 lists total calculation time required for a calculation. It is a rough evaluation and the values can be shorter by optimizing input data. In all the case except AP11276, more than 90% of the time is spent for the self-shielding calculation. In the standard level calculation, calculation times are the same between APOLLO2 and SLAROM-UF.

[*1](n,3n) reaction term should be multiplied by 2, but not applied here for lack of data.

Table 4.1 Summary of k-infinity and macroscopic reaction rate ratio

Cal. type	k-infinity	(Production term) / (Absorption term Etotal)		
		Ehigh[b)]	Elow[b)]	Etotal
MVP[a)]	1.31769 (±5)	0.89899 (±68)	0.41866 (±6)	1.31765 (±69)
TRIPOLI[a)]	1.31786 (±31) (+13)	0.89786 (±15) (-86)	0.42004 (±12) (+105)	1.31790 (±19) (+19)
AP172	1.32179 (+311)	0.89984 (+64)	0.42196 (+250)	1.32179 (+315)
SLA172	1.32520 (+570)	0.90439 (+410)	0.42079 (+162)	1.32519 (+572)
SLA172JFS	1.31849 (+61)	0.90059 (+122)	0.41788 (-59)	1.31847 (+63)
AP1968	1.31912 (+109)	0.89707 (-146)	0.42206 (+259)	1.31913 (+113)
SLA1968	1.31888 (+90)	0.89861 (-29)	0.42025 (+121)	1.31886 (+92)
AP11276	1.31833 (+49)	0.89590 (-235)	0.42244 (+287)	1.31834 (+53)
UF900	1.31820 (+38)	0.89723 (-133)	0.42096 (+175)	1.31819 (+42)

a) Number of neutron tracked: MVP 20,000(per batch) ×1,550(50 discard), TRIPOLI 10,000(per batch) ×1,200(21 discard)
b) Ehigh≥ $40.9keV$, Elow≤ $40.9keV$, Etotal=Ehigh+Elow
Values in parentheses (in pcm):
MVP: Statistical error(1σ)
TRIPOLI: Statistical error(1σ), (Difference from corresponding MVP value) / MVP Etotal
The others: (Difference from corresponding MVP value) / MVP Etotal

Table 4.2 Summary of macroscopic reaction rate

Cal. type	Production term ($\times 10^{-3}$)			Absorption term ($\times 10^{-3}$)		
	Ehigh	Elow	Etotal	Ehigh	Elow	Etotal
MVP	6.0319 (±6)	2.8090 (±5)	8.8410 (±8)	3.3152 (±31)	3.3945 (±6)	6.7097 (±32)
TRIPOLI	6.0262 (±11)(-64)	2.8192 (±8)(+115)	8.8454 (±14)(+50)	3.3149 (±7)(-5)	3.3969 (±12)(+36)	6.7117 (±14)(+31)
AP172	6.1016 (+788)	2.8612 (+590)	8.9628 (+1379)	3.3561 (+609)	3.4247 (+451)	6.7808 (+1060)
SLA172	6.1159 (+950)	2.8456 (+413)	8.9614 (+1363)	3.3524 (+555)	3.4100 (+231)	6.7624 (+786)
SLA172JFS	6.0612 (+332)	2.8124 (+38)	8.8737 (+370)	3.3284 (+197)	3.4019 (+110)	6.7303 (+308)
AP1968	6.0209 (-125)	2.8328 (+269)	8.8537 (+144)	3.3125 (-40)	3.3993 (+72)	6.7117 (+31)
SLA1968	6.0322 (+3)	2.8210 (+135)	8.8532 (+138)	3.3179 (+40)	3.3949 (+6)	6.7128 (+46)
AP11276	6.0137 (-206)	2.8356 (+300)	8.8493 (+94)	3.3111 (-61)	3.4013 (+102)	6.7124 (+41)
UF900	6.0279 (-46)	2.8282 (+216)	8.8561 (+171)	3.3139 (-19)	3.4044 (+148)	6.7183 (+129)

Values in parentheses (in pcm): same as Table 4.1.

Table 4.3 Calculation CPU time (sec)

Cal. type	AP172	SLA172	AP1968	SLA1968	AP11276	UF900
Hetero. cell	2	2	194	35	15,200	45
Homo. cell	2	2	160	18	13,500	24

Machine: CPU Pentium 4 2.40GHz, memory 500MByte free

5. Discussion

The results are investigated in each calculation level as itemized below. In addition to a general comparison, discussions are made on topics expected from theoretical consideration. The typical data of the self-shielding factor, the key quantity in the present work, are summarized in Appendix A.

1 Comparison on the reference level calculation (AP11276 and UF900)

2 Comparison on the 2nd reference level calculation (AP1968 and SLA1968)

a. Resonance overlap effect:
The 1968 group structure is not so fine as those in AP11276 and UF900 in the resolved resonance energy range of heavy nuclides. Its influence is evaluated quantitatively by comparing cross sections of ^{239}Pu and ^{238}U between the two reference level calculations.

3 Comparison on the standard level calculation (AP172 and SLA172)

a. Effect of heterogeneous-homogeneous equivalence:
SLAROM-UF uses the larger approximation in treating heterogeneous cell by the Tone method. Its influence is evaluated by comparing cross sections for the two cell models.

4 Comparison on the SLAROM-UF original standard level calculation (SLA172JFS)

a. Comparison among methodologies to create the self-shielding table
There is a difference in the methodologies to create the self-shielding table between APOLLO2 and SLAROM-UF standard libraries. The APOLLO2 library is based on the flux calculator, while the SLAROM-UF library is on the NR approximation and TIMS. Accuracy is investigated among the methodologies.

b. Effect of weight function
SLA172JFS shows better accuracy in the 172 group structure. Among special features of the library used in SLA172JFS, the effect of the better smooth function (weight function) is evaluated.

c. Effect of background cross section iteration
In the present work, an iteration procedure are not employed for the background cross section, by which resonance overlap effects are taken into account approximately. The effect is investigated using the results of SLA172JFS.

5.1 Comparison on the reference level calculations (AP11276 and UF900)

Figure 5.1.1 compares differences from the reference values on the fission reaction rate, the capture reaction rate, and the neutron spectrum. The left figures are on the relative difference and the right on the absolute difference. The absolute values correspond to those in the parentheses in Table 4.2, that is, a difference from MVP value is divided by the MVP energy total production or absorption reaction rate.

The results are satisfactory in that all the relative differences are within 1% and the absolute errors of reaction rates do not exceed 20 pcm in any energy group, except for the three points below:

1 Overestimation of the fission reaction rate around 4 keV in AP11276 and UF900 (discussed in Section 5.1.1)
The overestimation results in an error of several hundred pcm in the Elow component of the production and absorption terms in Table 4.2 (the fission reaction rate to be multiplied by the value of $\nu(\approx 3)$ for the values to be related to the production term).

2 Underestimation of neutron spectrum above 1 MeV in AP11276 (discussed in Section 5.1.2)
The underestimation results in an error of 200 pcm in the Ehigh component of the production term. The error appears by more than -100 pcm in the Ehigh component of the k-infinity.

3 Underestimation of neutron spectrum around 50 keV in UF900 (discussed in Section 5.2.4)
The underestimation is negligible in the relative difference but clear in the absolute difference, resulting in an error of 80 pcm in the absorption term. The error does not appear in the k-infinity due to a cancellation between the two reaction terms.

The above results indicate that AP11276 has good accuracy thanks to a cancellation of the independent errors between the Ehigh and Elow components. If one of the errors is corrected, the accuracy of the k-infinity will be deteriorated.

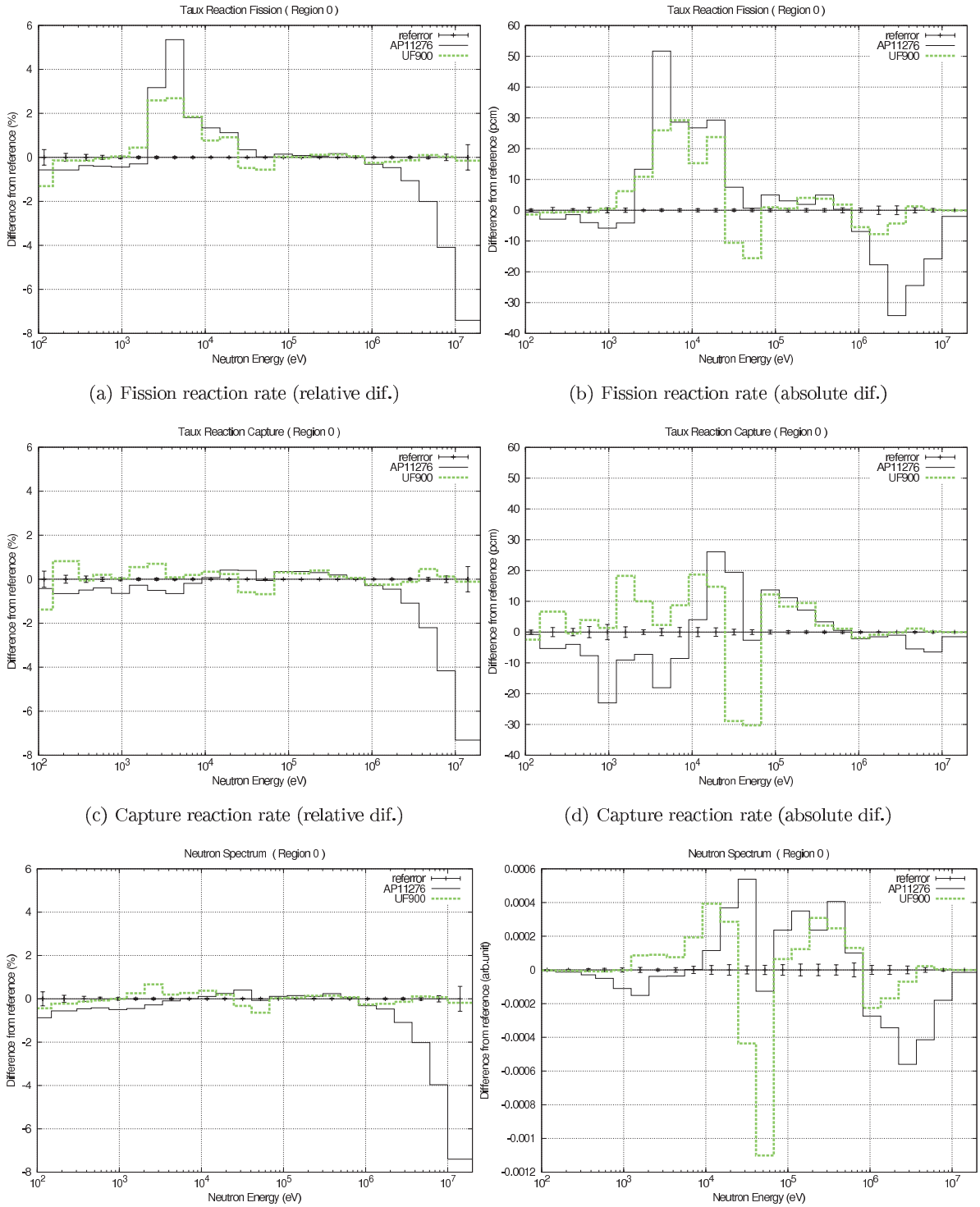

(a) Fission reaction rate (relative dif.)

(b) Fission reaction rate (absolute dif.)

(c) Capture reaction rate (relative dif.)

(d) Capture reaction rate (absolute dif.)

(e) Neutron spectrum (relative dif.)

(f) Neutron spectrum (absolute dif.)

Fig. 5.1.1 Accuracy of the reference level calculations

5.1.1 Overestimation of fission reaction around 4 keV

Figure 5.1.2 compares the cell-averaged effective microscopic cross sections of ^{239}Pu fission in the 172g structure. The result by TRIPOLI is also plotted. The left is on the heterogeneous benchmark model and the right is on a special homogeneous model in which the ^{239}Pu density was reduced to 1.0×10^{-10} (barn·cm) (instead the ^{240}Pu density was increased by 1.38×10^{-2} (barn·cm) to roughly compensate reactivity loss). In this modeling, the self-shielding effect on the ^{239}Pu cross section becomes negligible.

In AP11276 and TRIPOLI4, the difference from the reference exceeds 30% at the 50th group (3.35-3.53 keV) in both models. The error comes from not in the self-shielding treatment but in the infinite dilution cross section.

Figures 5.1.3-5.1.6 compare ^{239}Pu fission cross sections in a very fine energy mesh structure for the diluted ^{239}Pu model. Data for ENDF in each figure were taken from NJOY UNRESR module output at 300K. Data for MVP and TRIPOLI4 were obtained by tallying in the energy structure defined in the MVP library (within a statistical uncertainty of 1%), those for AP11276 were taken in its library energy structure, and those for UF900 were from PENDF (this case only at 270 K). AP11276 data include those self-shielded by the sub-group method and not self-shielded.

The results by MVP and AP11276(no self-shielding) follow the ENDF data. The other data fluctuate statistically and are difficult to see their adequacy.

Then the values are simply averaged in energy (Table 5.1.1). The averages for 3.35-3.53 keV and for 3.53-5.00 keV correspond to the controversial energy groups in Fig. 5.1.2. The group 51 (2.25-3.35 keV) was not compared since it is partly in the resolved resonance range (~2.5 keV). The averages for 3-4 keV and for 4-5 keV correspond to those described in the original ENDF file of JEFF-3.1. The ENDF data averaged here are identical to those in the original ENDF file (change in values by temperature rise is negligible).

MVP and AP11276 (no self-shielding) reproduce the ENDF data. UF900 gives slightly different results. The difference is mainly in interpolation schemes of cross section data. In SLAROM-UF library, PENDF is created with RECENT code of PREPRO2004, where the interpolation is carried out on the resonance parameters. On the other hand, the ENDF data is based on cross section interpolation. AP11276 (with self-shielding) and TRIPOLI4 do not reproduce the averaged values, which would come from CALENDF used to prepare the probability table.

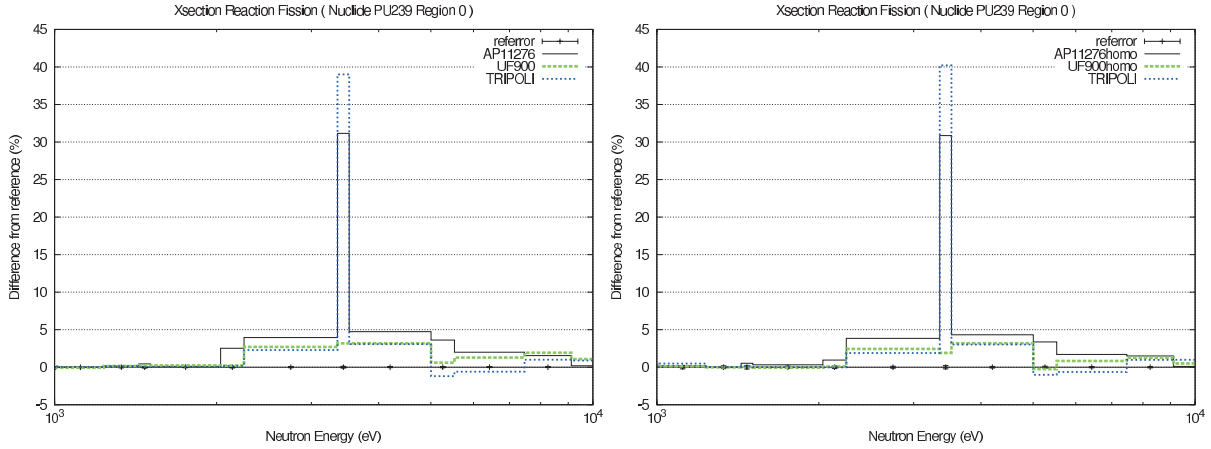

(a) Heterogeneous model

(b) Homogeneous model with diluted ^{239}Pu

Fig. 5.1.2 Accuracy of ^{239}Pu fission cross sections in an unresolved energy range (reference level cal.)

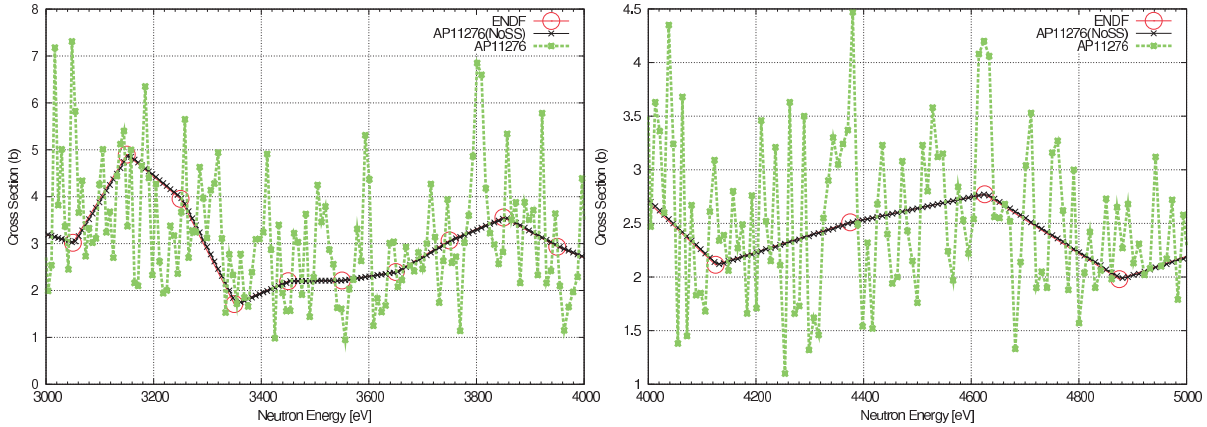

(a) from 3keV to 4keV (b) from 4keV to 5keV

Fig. 5.1.3 ^{239}Pu fission cross section in an unresolved energy range (AP11276 in Diluted ^{239}Pu model)

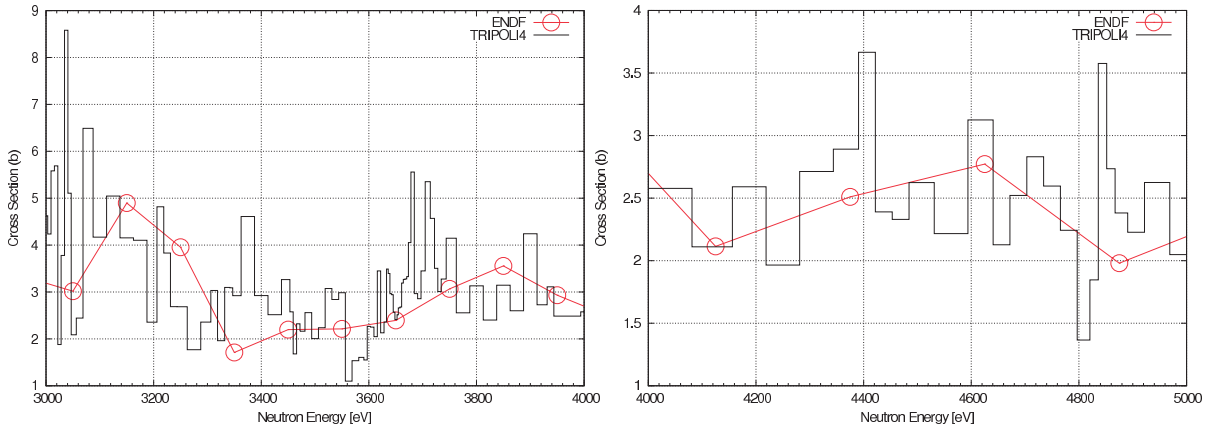

(a) from 3keV to 4keV (b) from 4keV to 5keV

Fig. 5.1.4 ^{239}Pu fission cross section in an unresolved energy range (TRIPOLI4 in Diluted ^{239}Pu model)

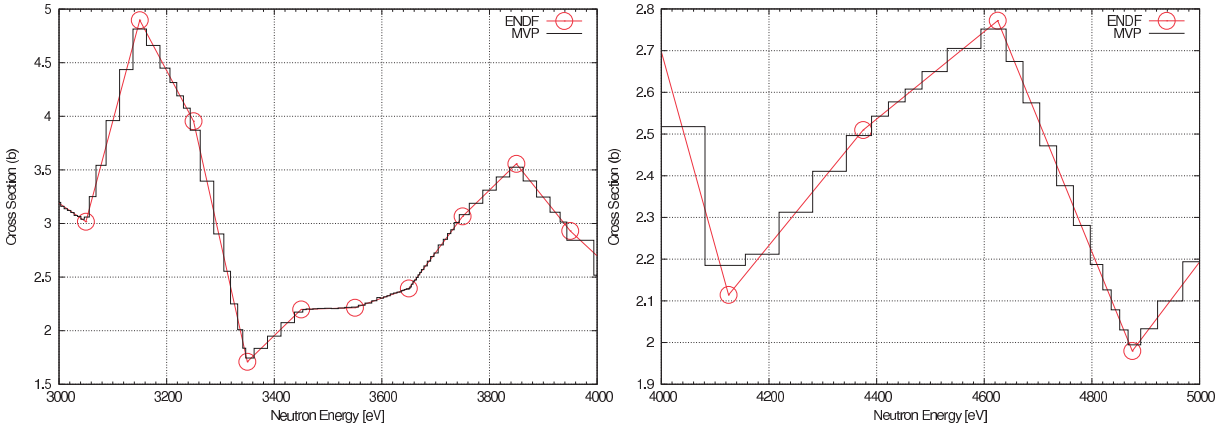

(a) from 3keV to 4keV (b) from 4keV to 5keV

Fig. 5.1.5 ^{239}Pu fission cross section in an unresolved energy range (MVP in Diluted ^{239}Pu model)

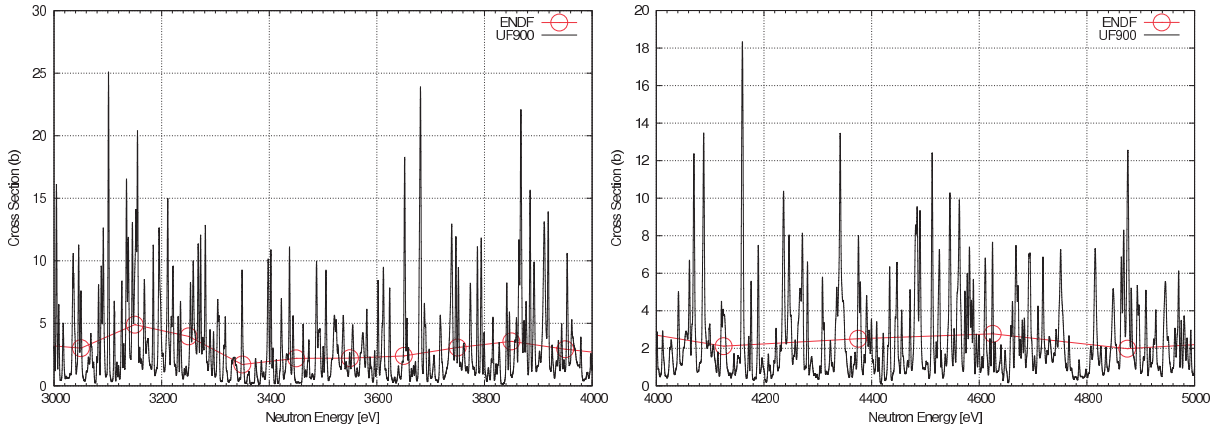

(a) from 3keV to 4keV (b) from 4keV to 5keV

Fig. 5.1.6 ^{239}Pu fission cross section in an unresolved energy range (UF900 in Diluted ^{239}Pu model)

Table 5.1.1 Average values of ^{239}Pu fission cross section in an unresolved energy range

Energy range (keV)	Data source					
	ENDF	AP11276 (noSS)	AP11276	TRIPOLI4	MVP	UF900
3.35-3.53 (AP172g, gp.50)	2.072	2.073 (+0.0)	2.721 (+31.3)	2.883 (+39.2)	2.071 (-0.0)	2.108 (+1.7)
3.53-5.00 (AP172g, gp.49)	2.541	2.542 (+0.0)	2.665 (+4.9)	2.626 (+3.3)	2.542 (+0.0)	2.605 (+2.5)
3-4	2.992	2.993 (+0.0)	3.181 (+6.3)	3.181 (+6.3)	2.992 (-0.0)	3.057 (+2.2)
4-5	2.394	2.395 (+0.0)	2.520 (+5.3)	2.485 (+3.8)	2.395 (+0.1)	2.428 (+1.4)

Values in parentheses (in %): difference to ENDF.

5.1.2 Underestimation above 1 MeV in AP11276

The underestimation is attributed to the incident energy of the fission spectrum. In APOLLO2, as the library is optimized to thermal reactor analyses, the incident energy is fixed at the lowest energy. On the other hand, SLAROM-UF uses an incident energy determined by a preliminary homogeneous calculation with an initial incident energy at 200 keV. When a fixed incident energy (determined by averaging with the weight function) is used in SLAROM-UF, a similar discrepancy arises (Fig. 5.1.7).

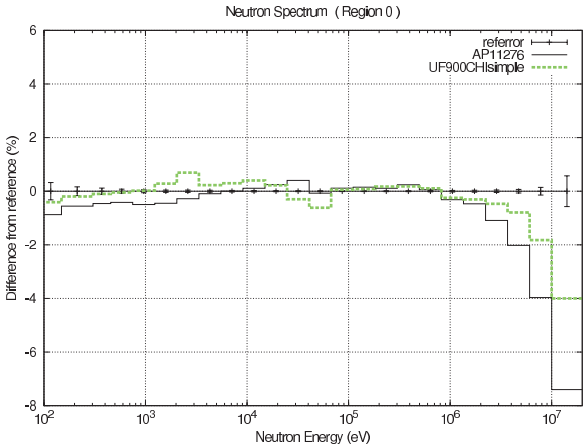

Fig. 5.1.7 Accuracy of neutron spectrum with fixed incident energy (UF900CHIsimple : UF900 cal. with the fixed incident energy for fission spectrum)

5.2 Comparison on the 2nd reference level calculations (AP1968 and SLA1968)

Calculation results are tabulated and plotted in the same fashion as in Section 5.1. A similar good accuracy is achieved as in the previous (1st) reference level calculations. Small differences observed are discussed in the following sections.

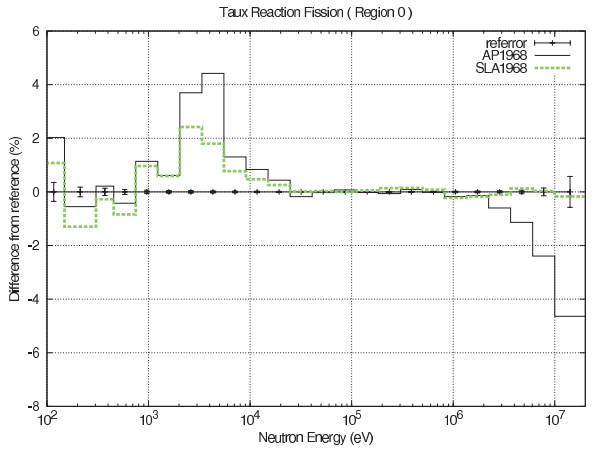

(a) Fission reaction rate (relative dif.)

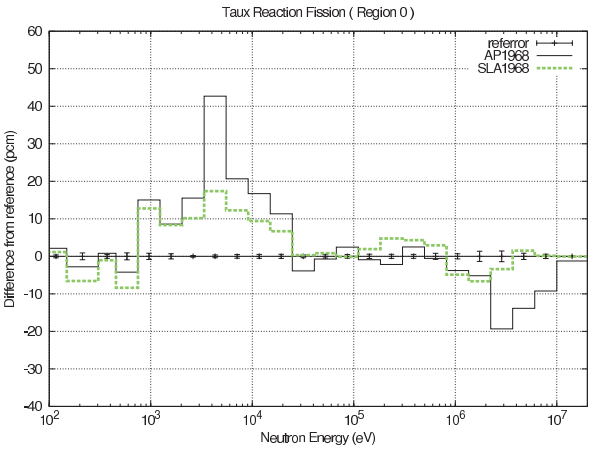

(b) Fission reaction rate (absolute dif.)

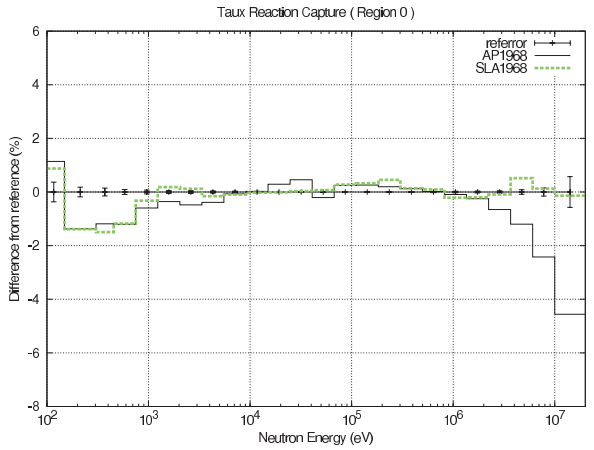

(c) Capture reaction rate (relative dif.)

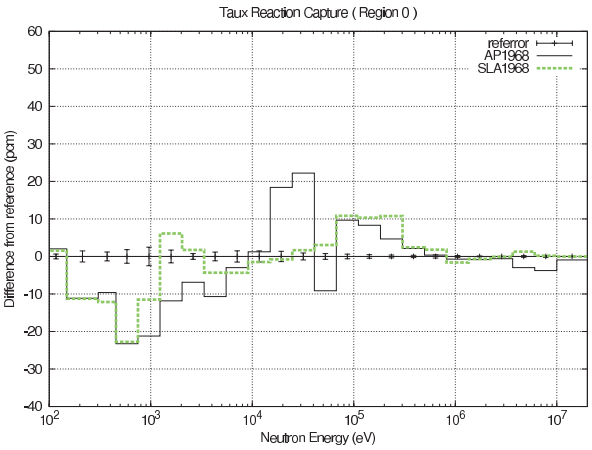

(d) Capture reaction rate (absolute dif.)

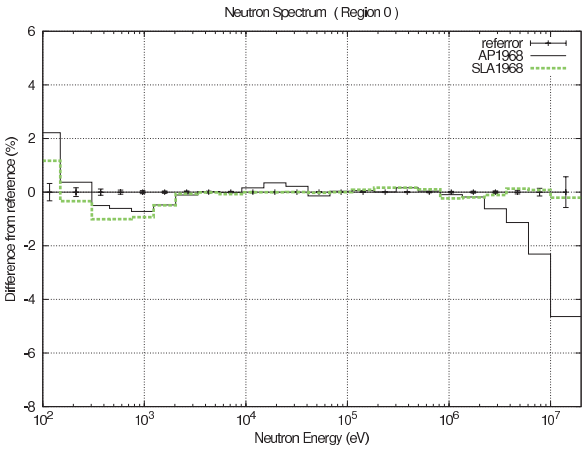

(e) Neutron spectrum (relative dif.)

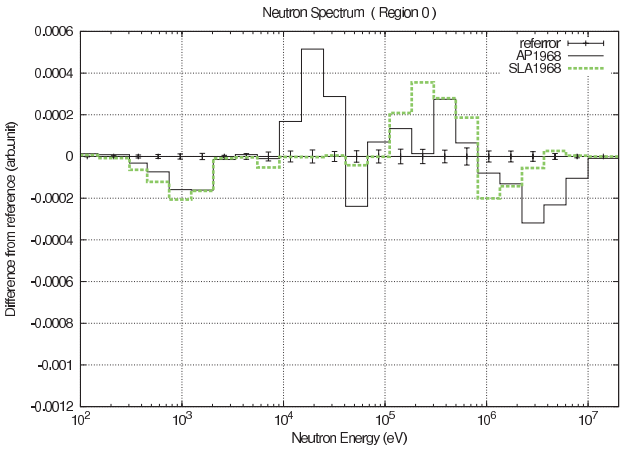

(f) Neutron spectrum (absolute dif.)

Fig. 5.2.1 Accuracy of the 2nd reference level calculations

5.2.1 Resonance overlap effect

Figure 5.2.2 compares cross sections of ^{239}Pu and ^{238}U between the 1st and 2nd reference level calculations for the homogeneous model in ECCO 33 or the 172 group structures.

The 1st reference level calculations both agree with the reference values within the statistical uncertainty below 2 keV (in the resolved resonance range). A few percents of differences are observed in the 2nd reference level calculations. It is due to the resonance overlap effect which the 1968 group calculation can not treat so accurately as in the 1st reference level calculation. The influence on the reaction rates is as small as about several ten pcm as observed in the comparison between Figs. 5.1.1 and 5.2.1.

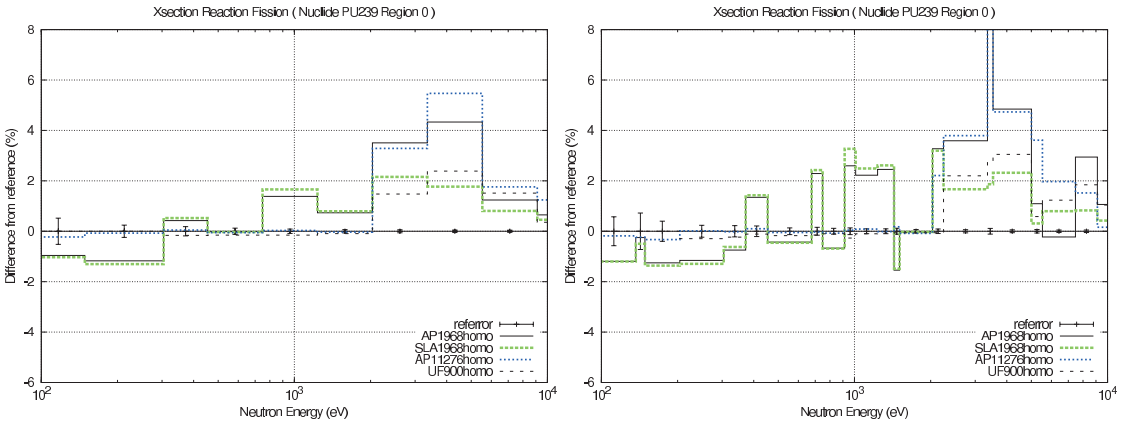

(a) ^{239}Pu fission (33g structure)

(b) ^{239}Pu fission (172g structure)

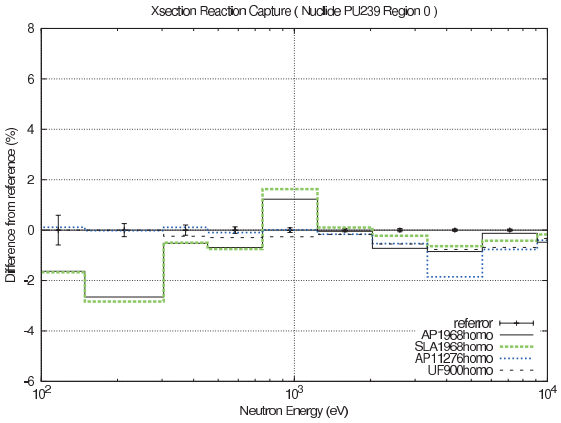

(c) ^{239}Pu capture (33g structure)

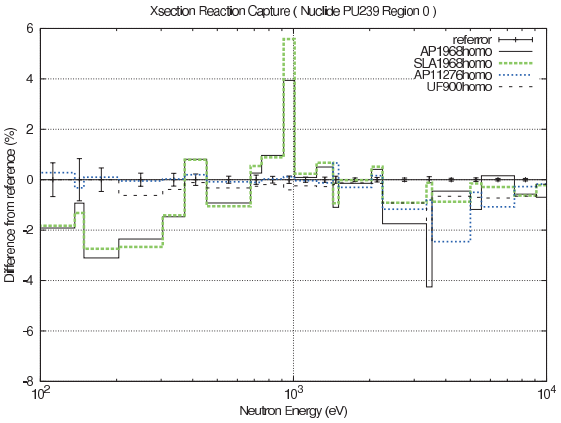

(d) ^{239}Pu capture (172g structure)

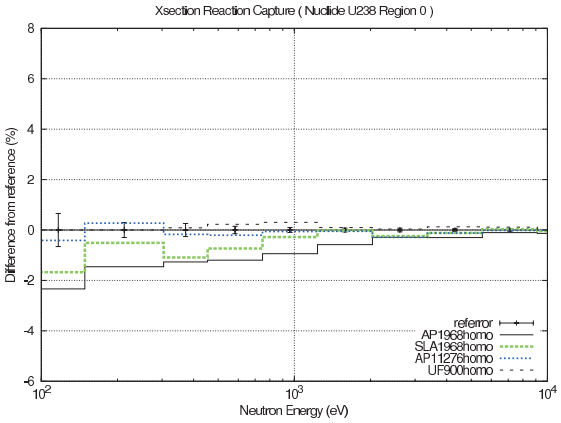

(e) ^{238}U capture (33g structure)

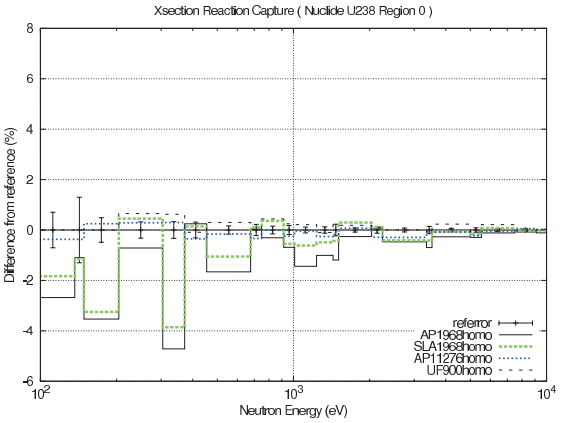

(f) ^{238}U capture (172g structure)

Fig. 5.2.2 Resonance overlap effect (1st and 2nd reference level calculations)

5.2.2 Overestimation of fission reaction around 4 keV

The overestimation mentioned in Section 5.1.1 appears similarly in the 1968 group calculation. The ^{239}Pu fission cross sections are compared similarly using the diluted ^{239}Pu model, in Table 5.2.1 and Figures 5.2.3-5.2.5.

Figure 5.2.3 is in the 172g structure and Figs.5.2.4 and 5.2.5 are in the 1968g structure. Data in the Table 5.2.1 is the simple average of the 1968g results. In Fig.5.2.5, PENDF data (at 270K, change in temperature is negligible) used in creation of the library is also plotted.

AP1968 data do not follow the ENDF data, which is the common behavior in the data based on CALENDF.

SLA1968 data show slight difference from the ENDF data (Fig.5.2.5). The difference originates from the same reason as mentioned in Section 5.1.1.

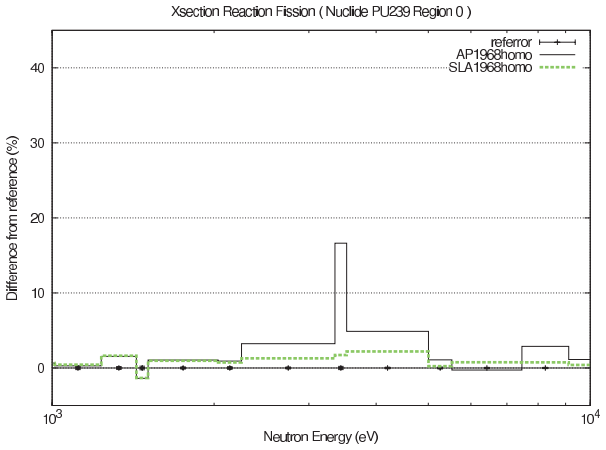

Fig. 5.2.3 Accuracy of ^{239}Pu fission cross section in an unresolved energy range (2nd reference level cal. in Diluted ^{239}Pu model)

Table 5.2.1 Average ^{239}Pu fission cross section in an unresolved energy range (1968 group library)

Energy range (keV)	Data source		
	ENDF	AP1968	SLA1968
3.35-3.53 (AP172g, gp.50)	2.072	2.467 (+19.1)	2.107 (+1.7)
3.53-5.00 (AP172g, gp.49)	2.541	2.664 (+4.8)	2.603 (+2.5)
3-4	2.992	3.147 (+5.1)	3.082 (+3.0)
4-5	2.394	2.493 (+4.1)	2.426 (+1.3)

Values in parentheses (in %): difference to ENDF.

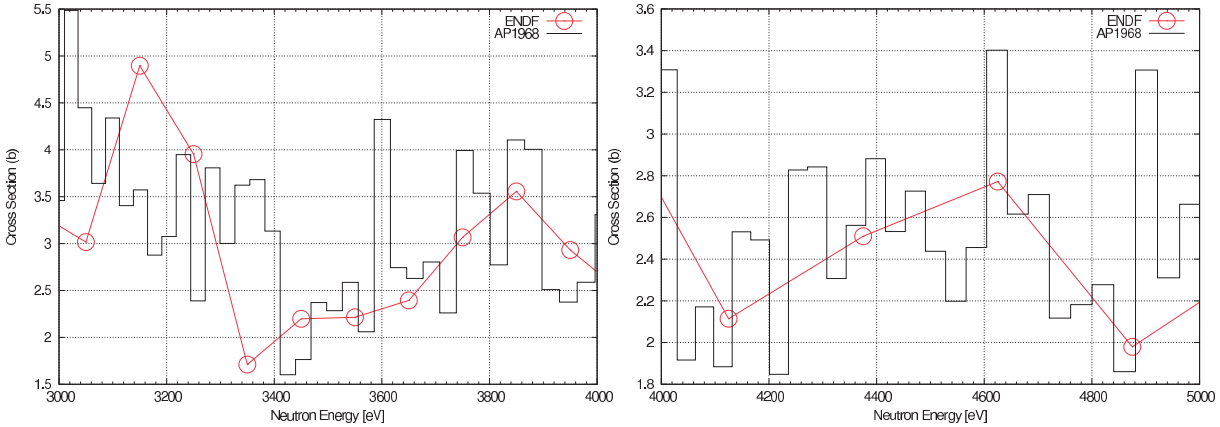

(a) from 3keV to 4keV (b) from 4keV to 5keV

Fig. 5.2.4 Diluted ^{239}Pu microscopic fission cross section in an unresolved energy (AP1968)

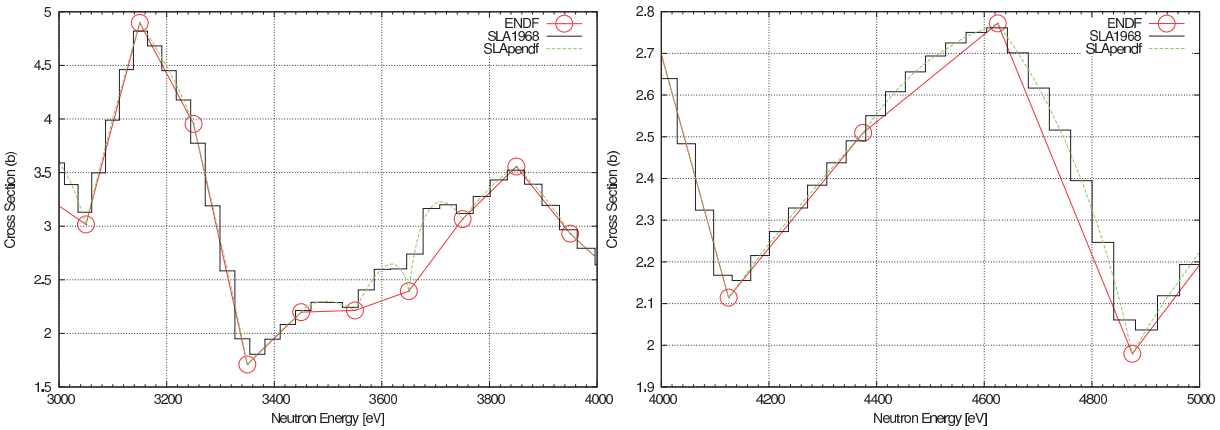

(a) from 3keV to 4keV (b) from 4keV to 5keV

Fig. 5.2.5 Diluted ^{239}Pu microscopic fission cross section in an unresolved energy (SLA1968)

5.2.3 Additional Comment on APOLLO2

Compared to Section 5.1.2, a small improvement is found on the effect of incident energy dependence of fission spectra. Fission spectra used in AP11276 and AP1968 are plotted with regard to SLA1968 in Fig. 5.2.6. The figure on the relative difference explains the difference observed in the neutron spectra between Figs. 5.1.1 and 5.2.1.

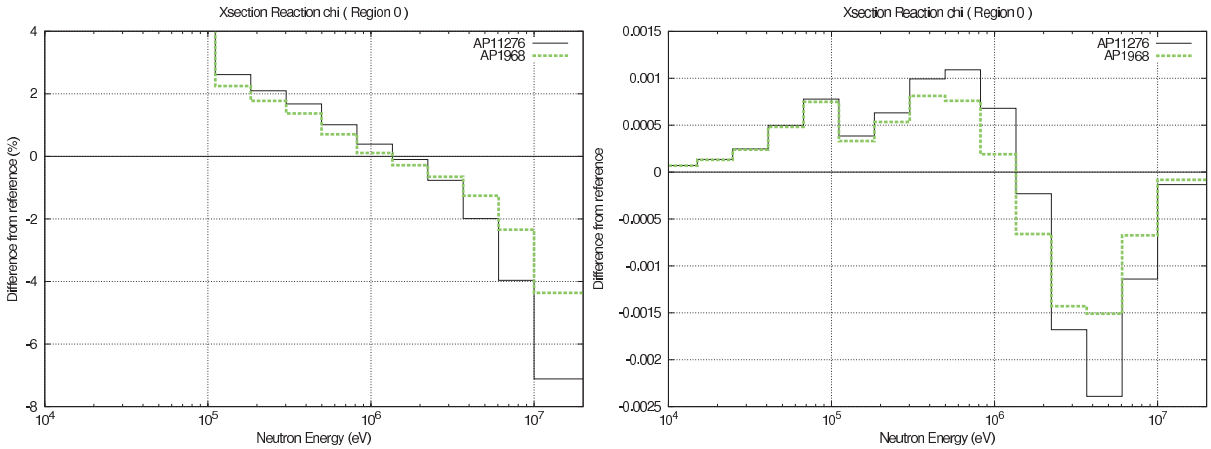

(a) Relative dif. (b) Absolute dif.

Fig. 5.2.6 Difference of fission spectrum between APOLLO2 reference level calculations (SLA1968 as reference)

In the absolute difference of the neutron spectrum, a discrepancy from the reference is clearly found from 10 to 100 (keV) in AP1968. It is observed in AP11276 of Fig. 5.1.1 as well. The discrepancy mainly originates from the scattering cross section of ^{23}Na (Fig. 5.2.7). It exceeds several percents in the 1968 group structure (Fig. 5.2.8). In the figure, a AP1968 case without the sub-group calculation is also shown with the index, "NoSG", which gives a good accuracy because the self-shielding effect in the 1968 group structure is negligible in this energy range (see Appendix A). This result indicates that the problem would be in the sub-group parameter of ^{23}Na.

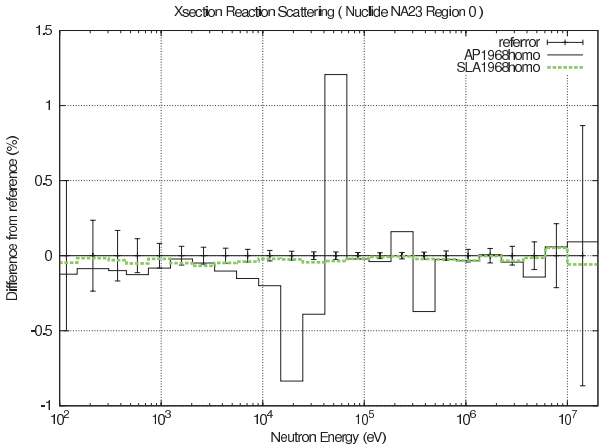

Fig. 5.2.7 Accuracy of ^{23}Na scattering cross section (1968 group cal.)

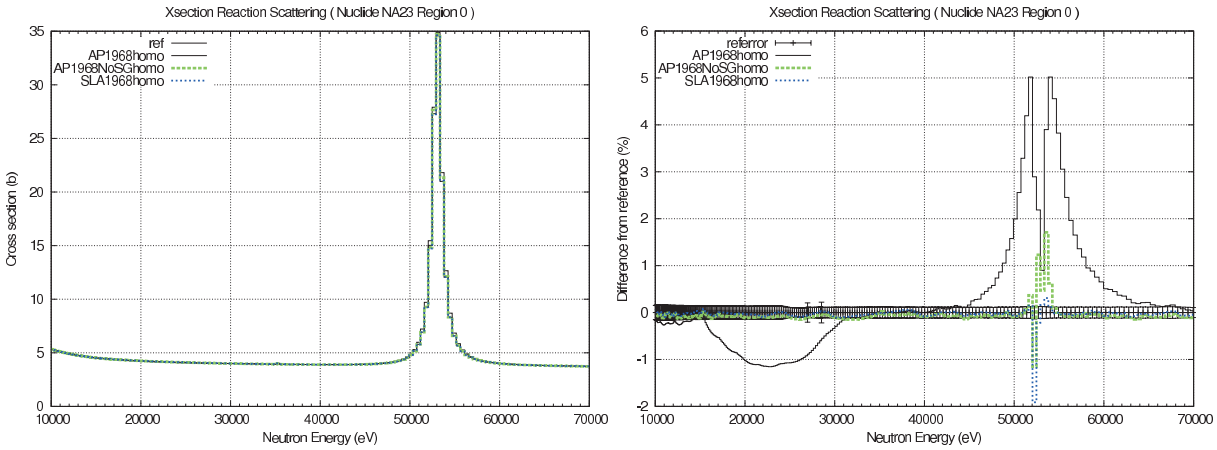

(a) Cross section (b) Relative dif.

Fig. 5.2.8 ^{23}Na scattering cross section in the 1968 group structure (1968 group cal.)

5.2.4 Additional Comment on SLAROM-UF

The neutron spectrum of SLA1968 shows better agreement around 40 keV than that of UF900.

Figure 5.2.9 plots the removal cross section of UF900 against SLA1968 in the 900 group structure (groups above 52 keV are partly condensed to have common energy group boundaries). The removal cross section here includes that of the inelastic scattering reaction. The difference appears below 52 keV where the cross section of UF900 is evaluated by the UF calculation. ^{56}Fe is the dominant contributor to the difference.

Figure 5.2.10 compares the removal cross section and PENDF of ^{56}Fe. The error appears in a smooth part of the cross section, thus the neutron spectrum should be determined mostly by external sources. The lack of fission and inelastic scattering sources in the UF calculation would be the reason of the error.

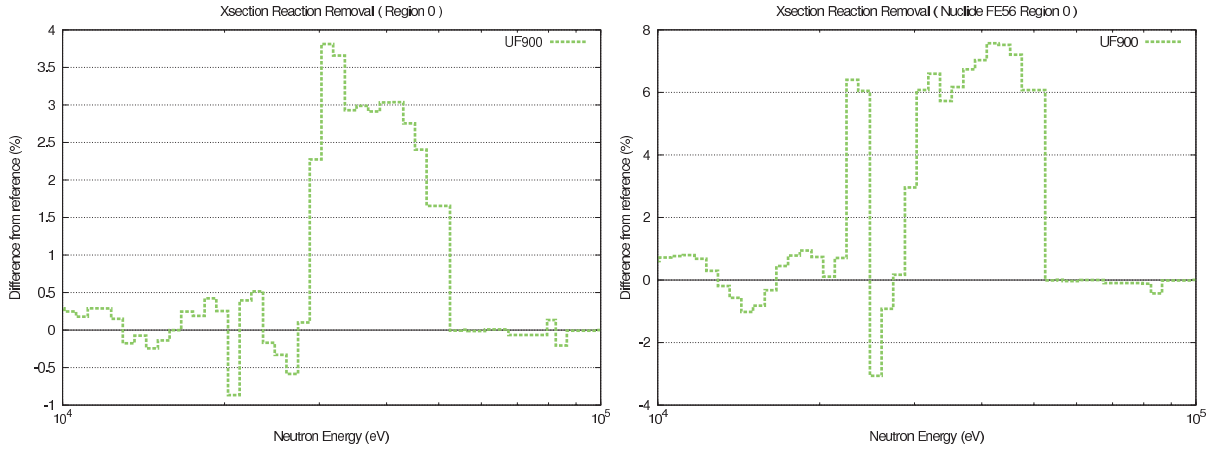

(a) Macroscopic (b) ^{56}Fe microscopic

Fig. 5.2.9 Accuracy of removal cross section in the 900 group structure (SLA1968 as reference)

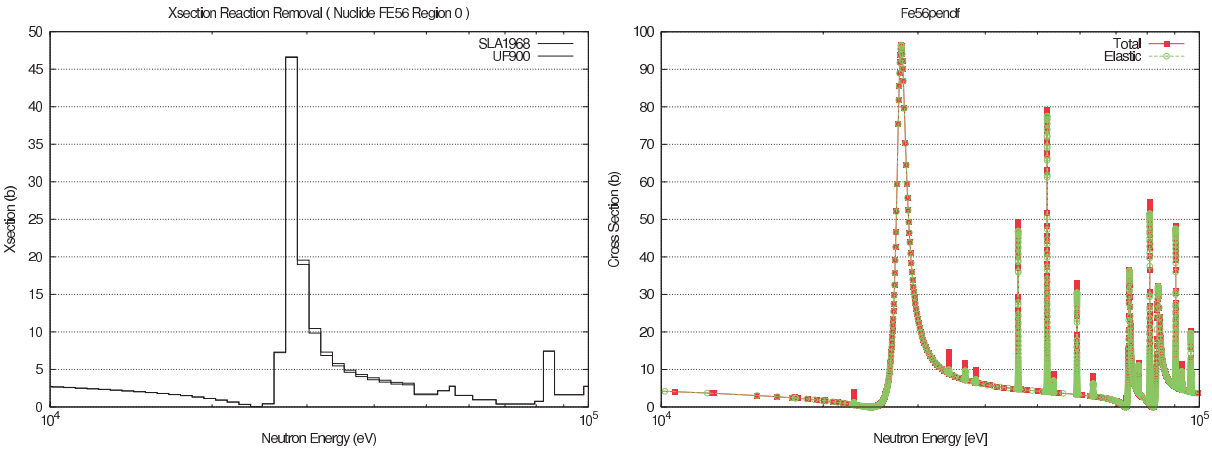

(a) Removal cross section (b) PENDF

Fig. 5.2.10 Removal cross section and pointwise cross section of ^{56}Fe

5.3 Comparison on the standard level calculations (AP172 and SLA172)

Figure 5.3.1 compares differences from the reference values on the reaction rates and neutron spectrum.

Apparently, errors are larger than those in the reference level calculations. The errors mainly come from those in the neutron spectrum.

Some differences exist between AP172 and SLA172, though the cross section libraries are created on a similar methodology, a reason of which will be discussed in Section 5.3.2.

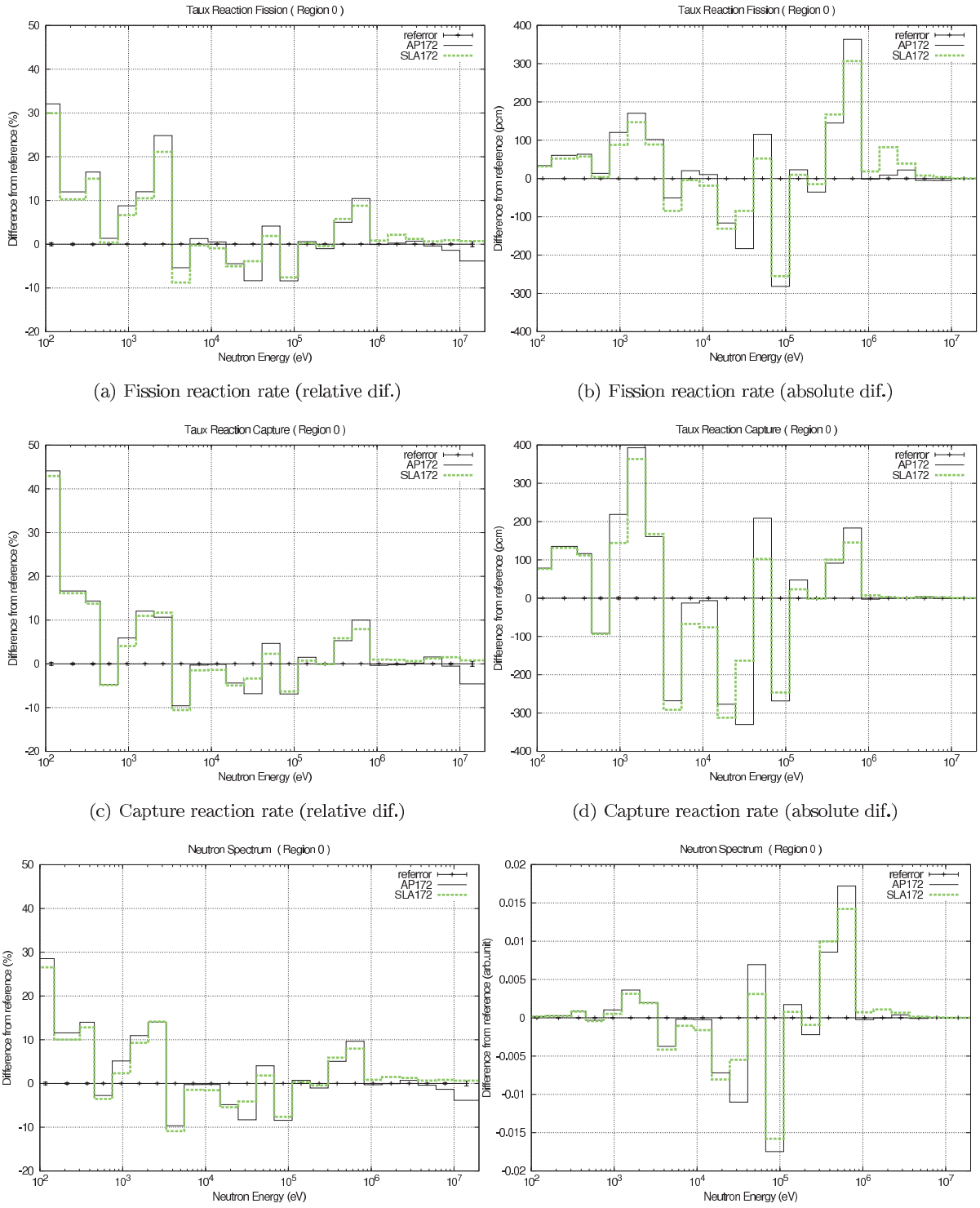

(a) Fission reaction rate (relative dif.)

(b) Fission reaction rate (absolute dif.)

(c) Capture reaction rate (relative dif.)

(d) Capture reaction rate (absolute dif.)

(e) Neutron spectrum (relative dif.)

(f) Neutron spectrum (absolute dif.)

Fig. 5.3.1 Accuracy of the standard level calculations

5.3.1 Effect of the heterogeneous-homogeneous equivalence

The SLA172 case uses the Tone method to evaluate the self-shielding effect in a heterogeneous cell, which would cause a larger error than the AP172 case. This influence is investigated by comparing cross sections of ^{239}Pu and ^{238}U between the heterogeneous and homogeneous models in Fig. 5.3.2.

The differences between SLA172 and AP172 are larger by several percents in the heterogeneous model for the ^{238}U capture cross section. It would be the errors accompanied with the Tone method.

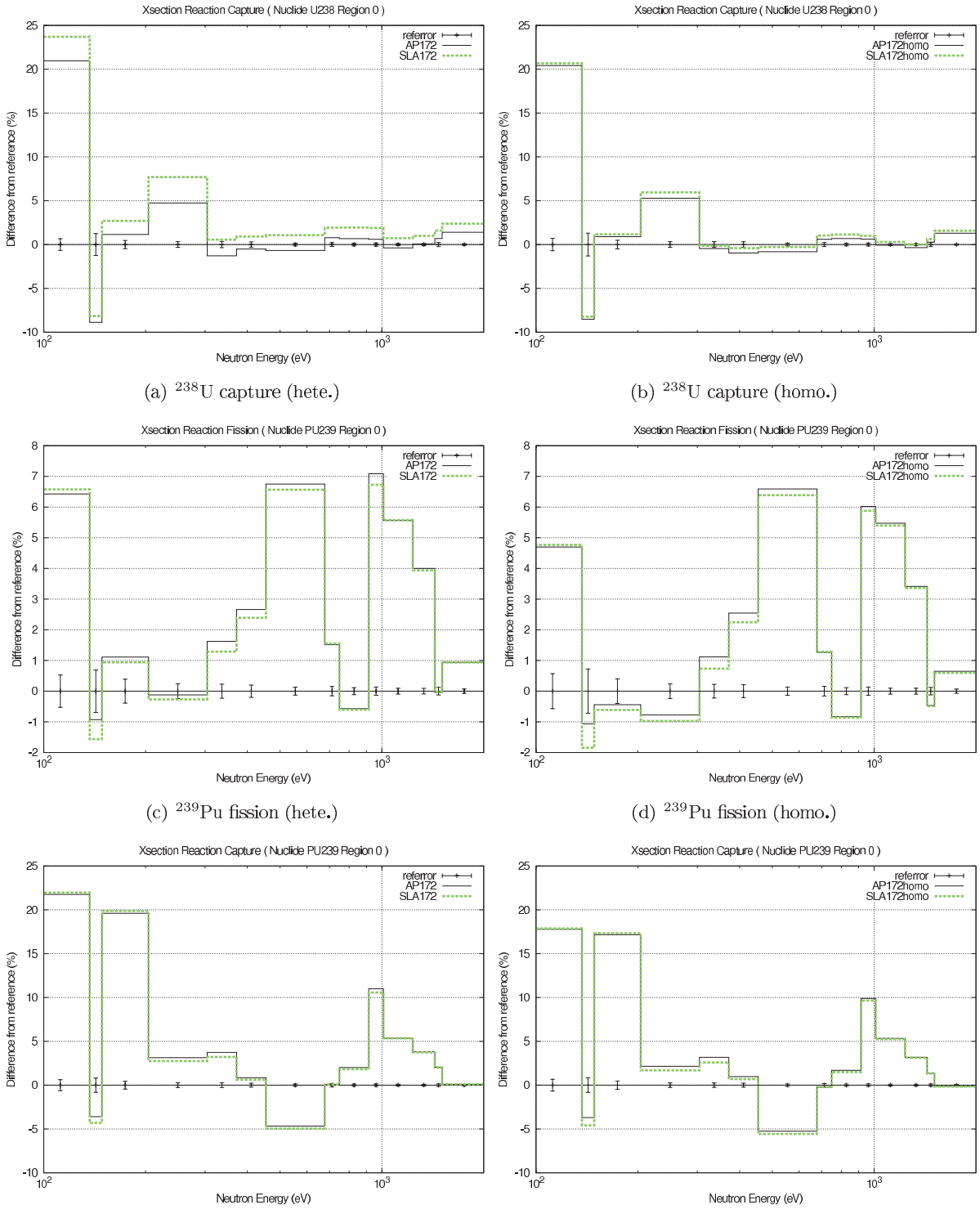

(a) ^{238}U capture (hete.)

(b) ^{238}U capture (homo.)

(c) ^{239}Pu fission (hete.)

(d) ^{239}Pu fission (homo.)

(e) ^{239}Pu capture (hete.)

(f) ^{239}Pu capture (homo.)

Fig. 5.3.2 Difference in accuracy of cross sections between heterogeneous and homogeneous calculations in the 172g structure

5.3.2 Other differences between AP172 and SLA172

Figure 5.3.3 compares macroscopic cross sections in the homogeneous model. Besides the differences in the fission cross section around 4 keV mentioned in Section 5.1.1, clear differences are observed in the scattering cross section. The differences similarly appear in the removal cross section, which causes the difference in the neutron spectrum. Figure 5.3.4 is on the absolute difference for the scattering cross section. We can see that the differences are mainly due to ^{56}Fe.

The difference of ^{56}Fe scattering cross section is attributed to a restriction on the background cross section (BG) in the AP172 case. In the APOLLO2 172 group library, the BG values for ^{56}Fe is truncated at 20 barn, because the behavior of the reaction rates against BG is not monotonous. On the other hand, actual BG in the benchmark problem is around 12 barn, making self-shielding factor calculated by AP172 erroneous.

This error can be removed by introducing the mixture self-shielding treatment into AP172 calculation as described in the next section.

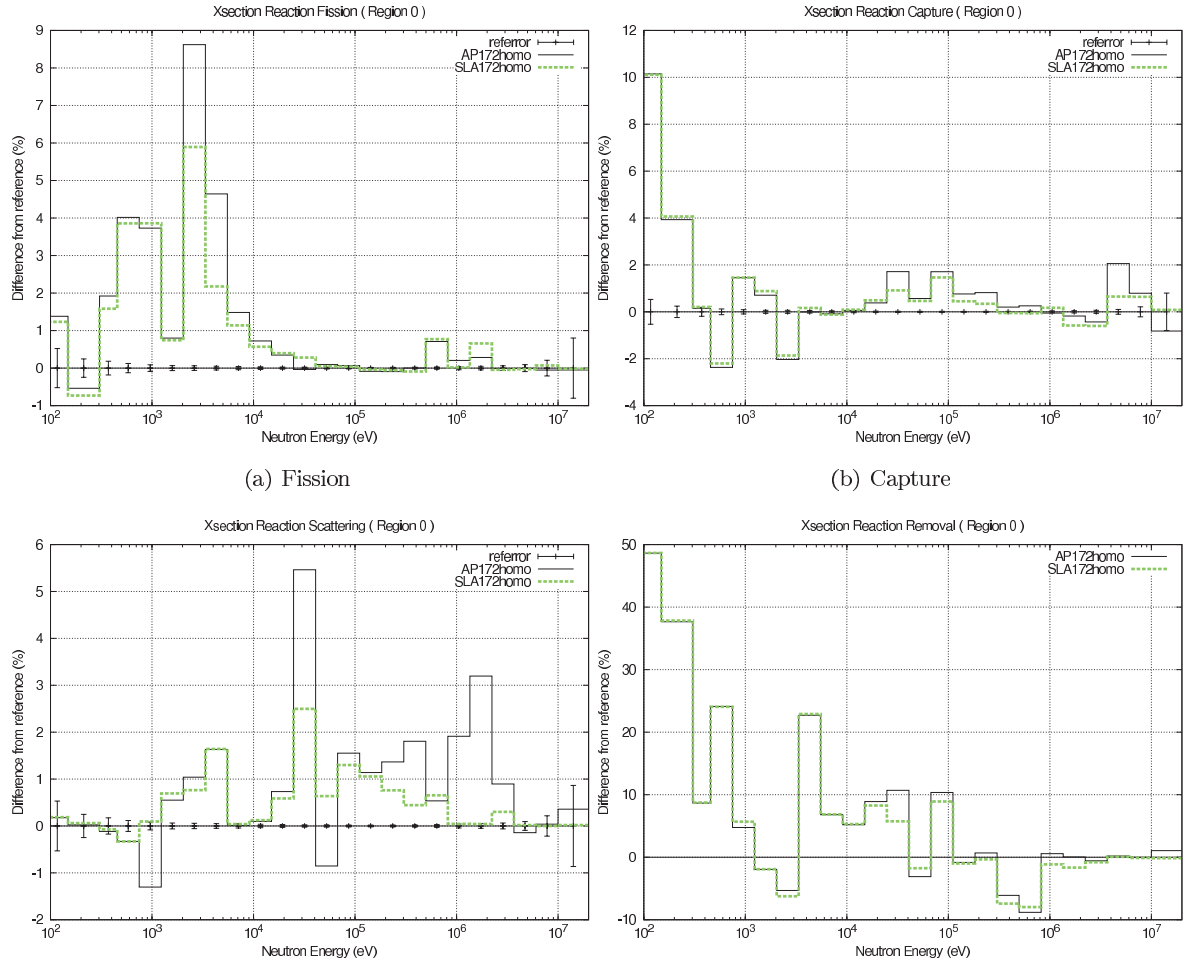

(a) Fission

(b) Capture

(c) Scattering

(d) Removal (SLA1968 as reference)

Fig. 5.3.3 Accuracy of macroscopic cross section (standard level homo cal.)

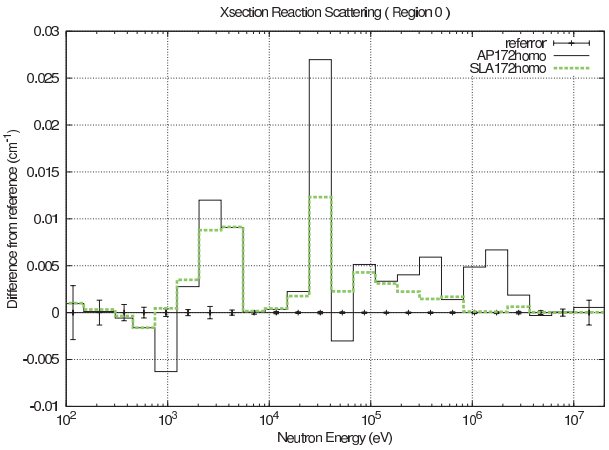

(a) Macroscopic (absolute dif.)

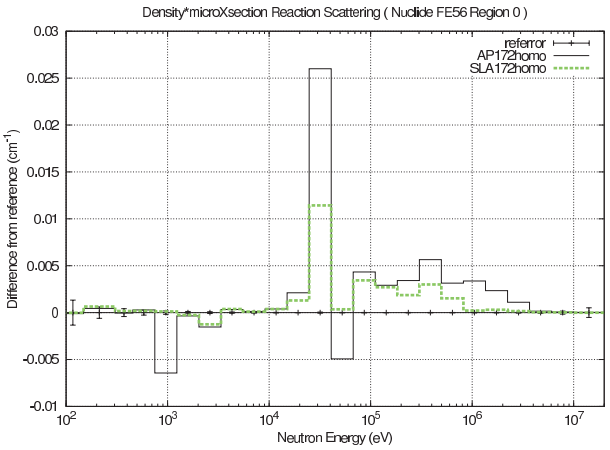

(b) ^{56}Fe micro * density (absolute dif.)

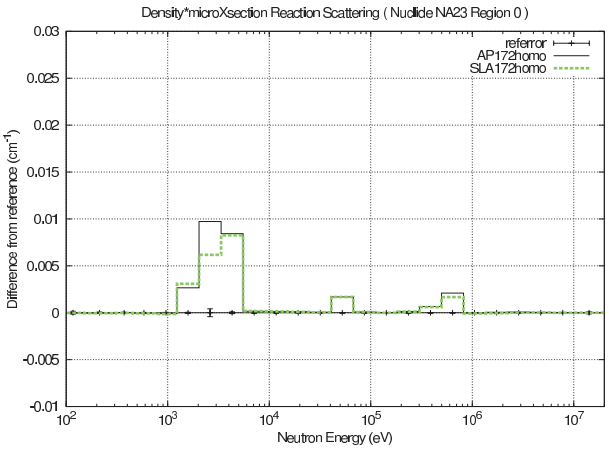

(c) ^{23}Na micro * density (absolute dif.)

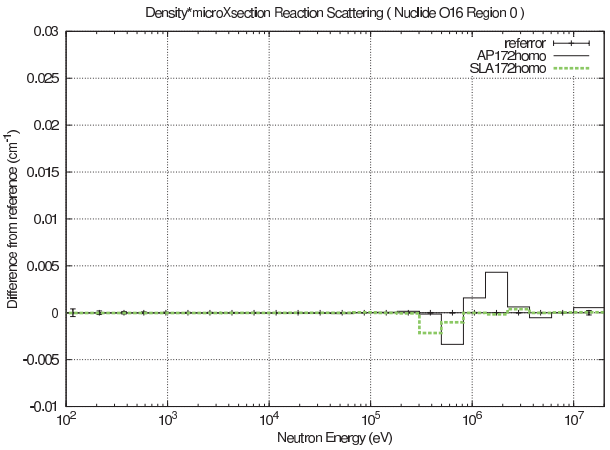

(d) ^{16}O micro * density (absolute dif.)

Fig. 5.3.4 Accuracy of scattering cross section (standard level homo cal.)

5.3.3 Application of mixture self-shielding treatment in AP172

The problem mentioned in Section 5.3.2 can be solved by introducing the mixture self-shielding (SS) treatment[14]. The mixture treatment calculates effective reaction rates for a BG value in the code.

In the mixture treatment, a homogeneous cell calculation is carried out in the AP11276 group structure for an energy range of interest. The slowing down equation is solved in a similar manner to the flux calculator of NJOY. Exceptions are

- the slowing down source term is expressed by the TR approximation,
- the probability table is used to evaluate a resonance integral,
- as many resonant isotopes as required can be handled.

The last feature is effective to treat the resonance overlap effects accurately. The reaction rate thus calculated for a background cross section is used in the multigroup equivalence step in place of the library created by NJOY.

The mixture treatment option is available in the standard APOLLO2; however, the restriction remains on the treatment of the self-shielding for the transfer matrix. Then APOLLO2 has been tentatively modified by M.Coste of CEA to treat the SS factor on the transfer matrix correctly and calculation on the present benchmark were performed using the slightly different nuclear data JEFF-3.2β.

Figure 5.3.5 compares the scattering cross sections between the new result (named "AP172mix") and the previous standard level result. In the comparison, a difference in nuclear data (between JEFF-3.1 and JEFF-3.2β) is negligible. We can see the error found in AP172 is successfully removed in AP172mix.

Small differences remain between SLA172 and AP172mix around 1 MeV in ^{56}Fe, and around 1 keV and 10 MeV in ^{16}O. Those in ^{56}Fe is because the self-shielding effect is not considered in AP172mix around the energy range, which will be solved easily by changing default setting. Those in ^{16}O newly appeared in AP172mix need an investigation.

An improvement is also expected in the resonance treatment for the heavy nuclides. Figure 5.3.6 compares cross sections of ^{239}Pu and ^{238}U. A difference due to the nuclear data is again negligible as shown in the right figures.

Improvement is clearly found in ^{239}Pu capture cross section and around 1 keV in ^{239}Pu fission cross section. The result is similar to that obtained with TIMS used in SLA172JFS which will be shown in Section 5.4.1.

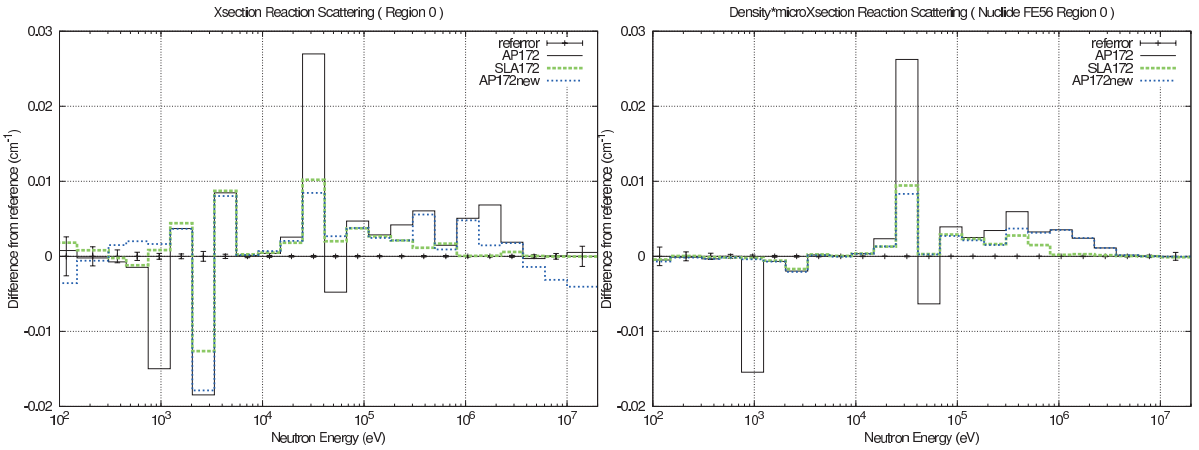

(a) Macroscopic (absolute dif.)

(b) ^{56}Fe micro*density (absolute dif.)

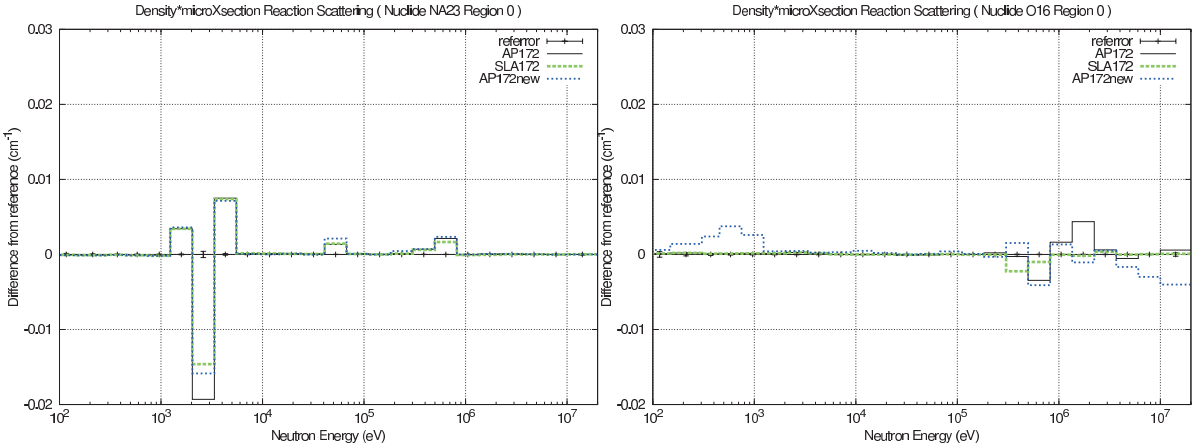

(c) ^{23}Na micro*density (absolute dif.)

(d) ^{16}O micro*density (absolute dif.)

Fig. 5.3.5 Improvement in scattering cross sections by AP172mix (standard level cal.)

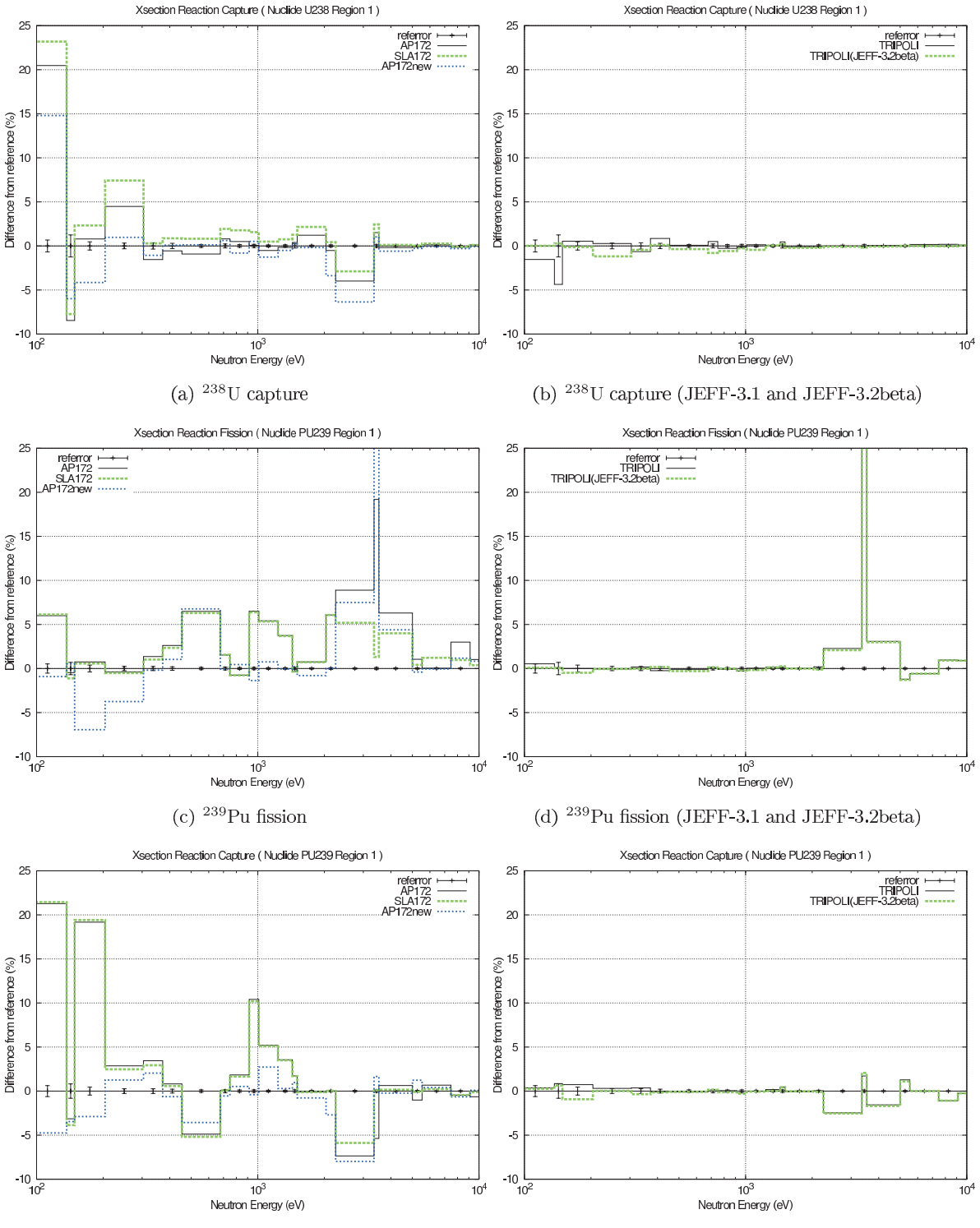

(a) ^{238}U capture

(b) ^{238}U capture (JEFF-3.1 and JEFF-3.2beta)

(c) ^{239}Pu fission

(d) ^{239}Pu fission (JEFF-3.1 and JEFF-3.2beta)

(e) ^{239}Pu capture

(f) ^{239}Pu capture (JEFF-3.1 and JEFF-3.2beta)

Fig. 5.3.6 Improvement of cross sections (in fuel region) for heavy nuclides by AP172mix (Statistical uncertainties of TRIPOLI results are similar to that of MVP result.)

5.4 Comparison on the SLAROM-UF original standard level calculation (SLA172JFS)

SLA172JFS uses the cross section library created using TIMS for ^{239}Pu and ^{238}U, and using the NR approximation and the weight function for the other nuclides.

The weight function (named here "JFSweight") is similar to the collision density calculated in SLA1968 (Fig. 5.4.1). The right figure compares the neutron spectra calculated with SLA172JFS and SLA172wt1968 (library was similarly created using collision density calculated in SLA1968). The similarity of the two collision densities indicates that JFSweight is an appropriate weight function for the present benchmark problem. One may think that the accuracy of the neutron spectrum in SLA172wt1968 is not satisfactory in spite of use of the "real" weight spectrum. The condition of Eq. (2.2.5) should be satisfied more strictly for further accuracy.

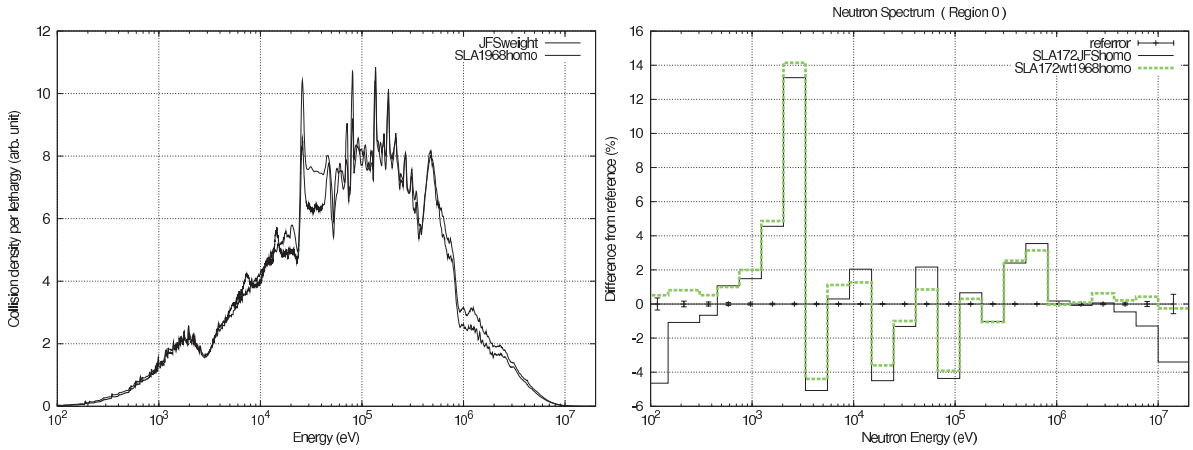

(a) Collision density (b) Neutron spectrum

Fig. 5.4.1 Comparison of collision density and resulting calculated neutron spectrum

The summary of the k-infinity calculations and reaction rates are again listed in Tables 5.4.1 and 5.4.2. The following new calculations were added to see a change in the transition.

SLA172JFSnoWT Library based on the $1/E + \chi$ weight function instead of "JFSweight" in SLA172JFS.

SLA172JFSnoWTnoR No R-factor in SLA172JFSnoWT.

The difference from SLA172 to SLA172JFSnoWTnoR comes from use of TIMS for ^{239}Pu and ^{238}U, and use of the NR approximation for the other nuclides, both instead of the flux calculator. As described later, differences between TIMS and the flux calculator are small and the latter change is the major contribution.

The difference from SLA172JFSnoWTnoR to SLA172JFSnoWT is use of the R-factor. The effect appears in the Elow terms.

The difference from SLA172JFSnoWT to SLA172JFS is use of JFSweight. This difference causes the largest impact and appears mainly in the Ehigh terms.

The results of SLA172JFS are plotted in contrast to SLA172 in Fig. 5.4.2. An improvement is found in general and mainly comes from that in the neutron spectrum.

Table 5.4.1 Transition from SLA172 to SLA172JFS on k-infinity and macroscopic reaction rate ratio

Cal. type	k-infinity	(Production term) / (Absorption term Etotal)		
		Ehigh	Elow	Etotal
SLA172	1.32520 (+569)	0.90439 (+410)	0.42079 (+162)	1.32519 (+572)
SLA172JFSnoWTnoR	1.32550 (+592)	0.90496 (+453)	0.42052 (+141)	1.32548 (+594)
SLA172JFSnoWT	1.32365 (+453)	0.90496 (+453)	0.41867 (+1)	1.32363 (+454)
SLA172JFS	1.31849 (+60)	0.90059 (+122)	0.41788 (-59)	1.31847 (+63)

Definition of the values follow Table 4.1.

Table 5.4.2 Transition from SLA172 to SLA172JFS on macroscopic reaction rate

Cal. type	Production term $(\times 10^{-3})$			Absorption term $(\times 10^{-3})$		
	Ehigh	Elow	Etotal	Ehigh	Elow	Etotal
SLA172	6.1159 (+950)	2.8456 (+413)	8.9614 (+1363)	3.3524 (+555)	3.4100 (+231)	6.7624 (+786)
SLA172JFSnoWTnoR	6.1029 (+803)	2.8359 (+304)	8.9388 (+1106)	3.3454 (+451)	3.3984 (+58)	6.7438 (+509)
SLA172JFSnoWT	6.0980 (+748)	2.8212 (+137)	8.9192 (+885)	3.3428 (+411)	3.3957 (+18)	6.7384 (+429)
SLA172JFS	6.0612 (+332)	2.8124 (+38)	8.8737 (+370)	3.3284 (+197)	3.4019 (+110)	6.7303 (+308)

Definition of the values follow Table 4.1.

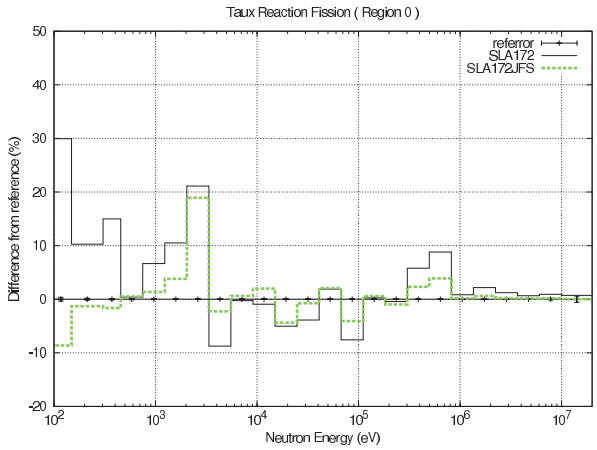

(a) Fission reaction rate (relative dif.)

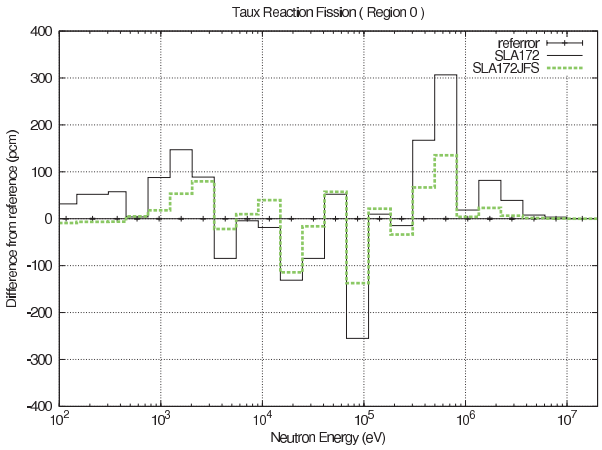

(b) Fission reaction rate (absolute dif.)

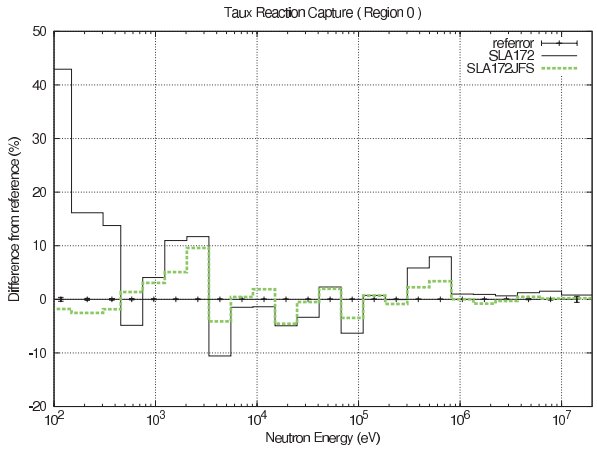

(c) Capture reaction rate (relative dif.)

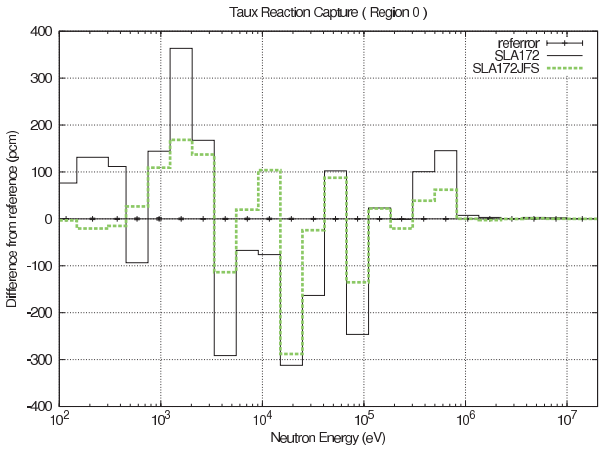

(d) Capture reaction rate (absolute dif.)

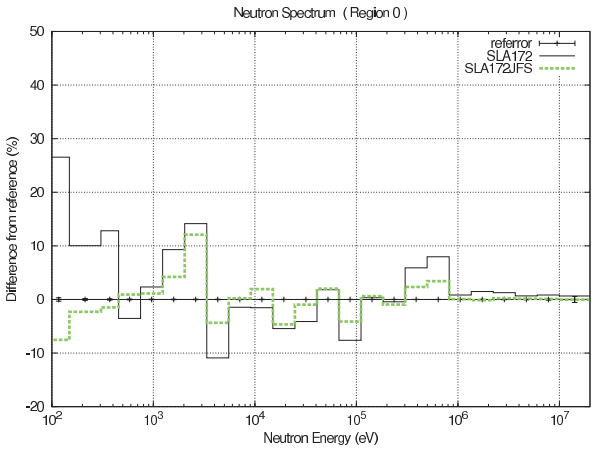

(e) Neutron spectrum (relative dif.)

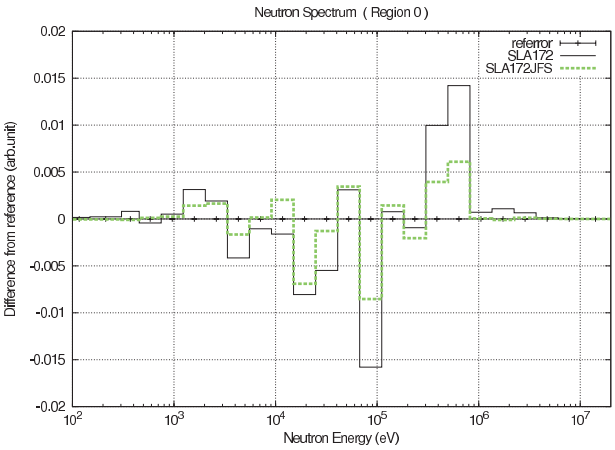

(f) Neutron spectrum (absolute dif.)

Fig. 5.4.2 Accuracy of the SLAROM-UF original standard level calculation

5.4.1 Comparison among methodologies to create the self-shielding tables

To understand the difference between SLA172 and SLA172JFS in more detail, methodologies used in creating the self-shielding tables are investigated.

Methodologies compared are

- SLA172 : the flux calculator of NJOY for all self-shielding factors
- SLA172NR : the NR approximation for all self-shielding factors
- SLA172JFS : TIMS for ^{239}Pu and ^{238}U and the NR approximation for the others.
- SLA172JFSnoR : TIMS without the R-factor in SLA172JFS, which ignores the resonance overlap effect between ^{239}Pu and ^{238}U[*1].

The comparisons are made on the homogeneous cell model and in the 172 group structure.

Figure 5.4.3 is on ^{239}Pu and ^{238}U. The left figures compare results based on the flux calculator (SLA172), TIMS without the R-factor (SLA172JFSnoR), and the NR approximation (SLA172NR).

It is observed that the NR approximation causes larger errors in ^{238}U capture cross section below 400eV. The result of the flux calculator is as good as that by TIMS without the R-factor.

The right figures show the R-factor effect (resonance overlap effect). The effect mainly appears in ^{239}Pu cross sections, which results are similar to those mentioned in Sections 5.2.1 and 5.3.3.

Figure 5.4.4 is on the scattering cross sections. Clear errors are observed around 3 keV in SLA172NR and around 30 keV in SLA172. The former is on the resonance of ^{23}Na and the latter is on the resonance of ^{56}Fe.

Use of the flux calculator is effective for ^{23}Na as in the above heavy nuclide cases; however, it is not true for ^{56}Fe and the NR approximation is better. Considering that the UF calculation, which solves a slowing down equation as in the flux calculator, does not yield this large error, lack of the contribution of the source term by the other isotopes, would be a cause of the error.

[*1] This case is equivalent to a flux calculator case with an admixture moderator by specifying the parameters; alpha2=0.875 $\left(= \frac{(30-1)^2}{(30+1)^2},\ 30 :\ \text{mass of admixture moderator}\right)$, sam=1.0, beta=1.0, and gamma=1.0 in NJOY GROUPR module.

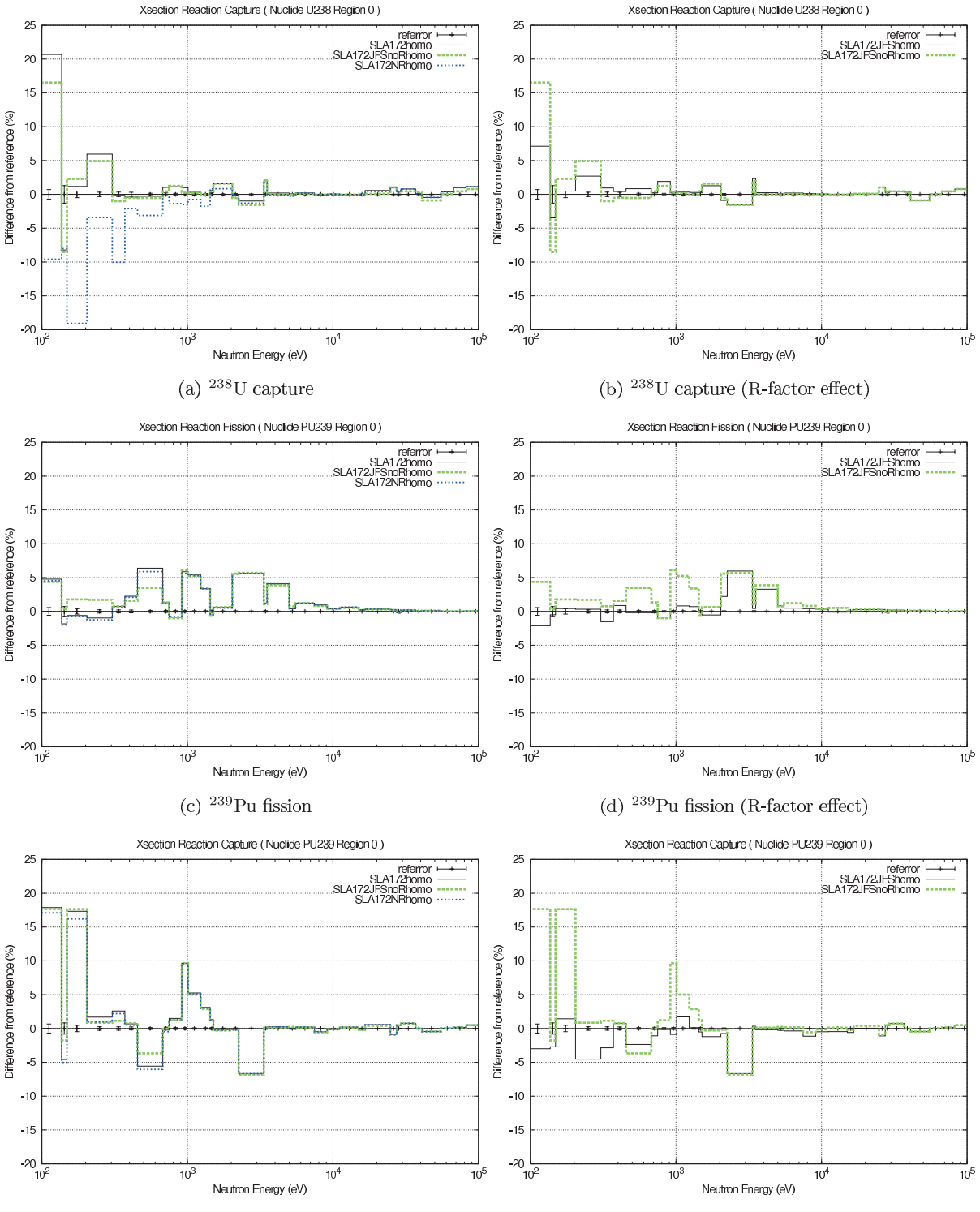

(a) ^{238}U capture

(b) ^{238}U capture (R-factor effect)

(c) ^{239}Pu fission

(d) ^{239}Pu fission (R-factor effect)

(e) ^{239}Pu capture

(f) ^{239}Pu capture (R-factor effect)

Fig. 5.4.3 Comparison of cross sections for heavy nuclides among various methodology in creating self-shielding table (standard level homo cal.)

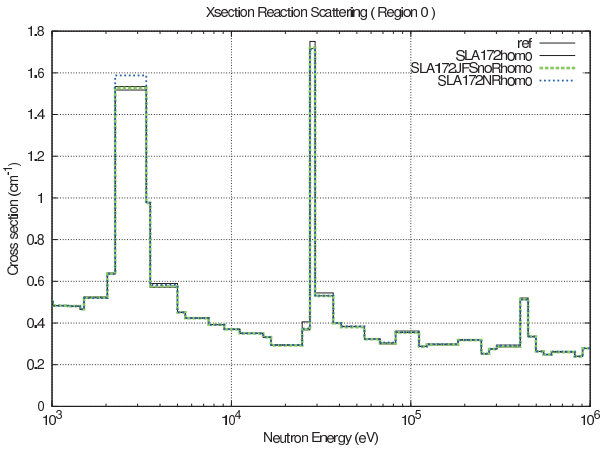

(a) Macroscopic scattering cross section

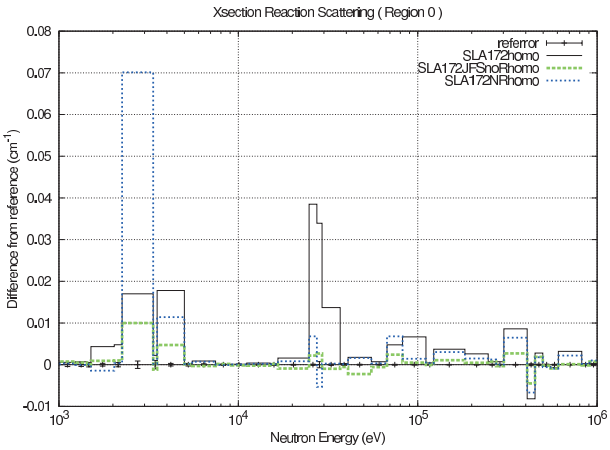

(b) Macroscopic scatteing cross section (absolute dif.)

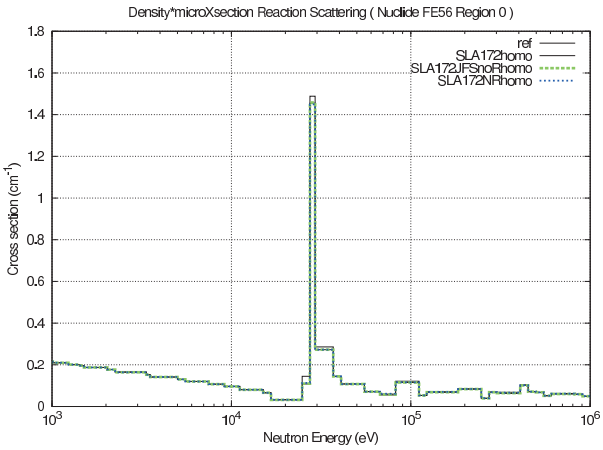

(c) Scattering cross section * density (^{56}Fe)

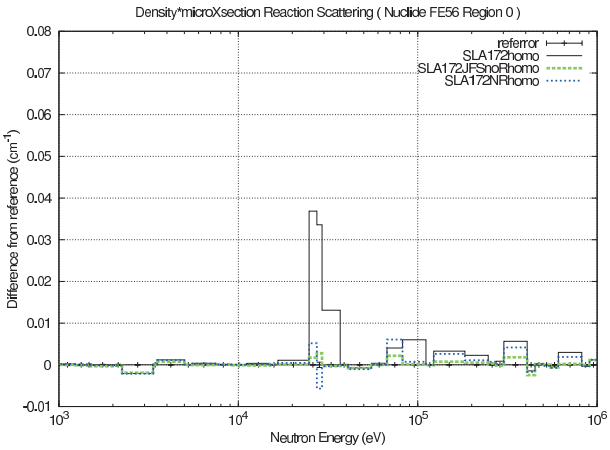

(d) Scattering cross section * density (^{56}Fe, absolute dif.)

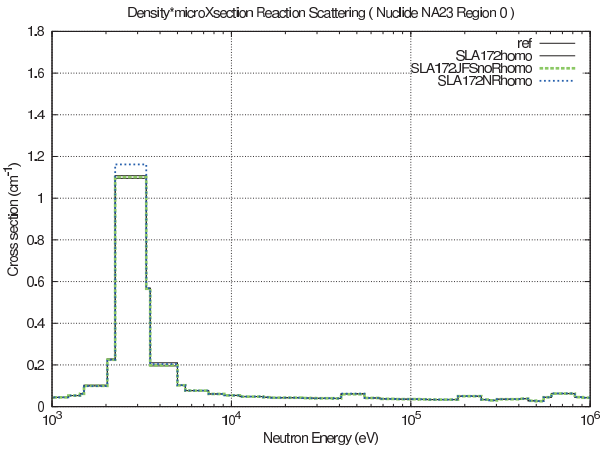

(e) Scattering cross section * density (^{23}Na)

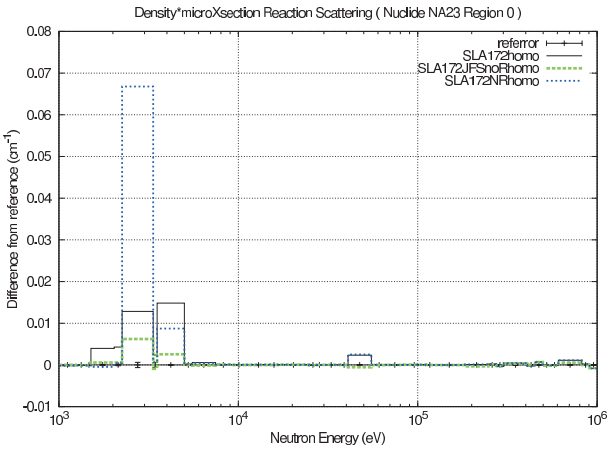

(f) Scattering cross section * density (^{23}Na, absolute dif.)

Fig. 5.4.4 Comparison of scattering cross sections among various methodology in creating self-shielding table
(standard level homo cal.)

5.4.2 Effect of weight function

The other difference between SLA172 and SLA172JFS is use of JFSweight. The effect mainly appears on the neutron spectrum which originates from the removal cross section as in Fig. 5.4.5. Contribution of nuclides are equally found in ^{16}O, ^{23}Na, and ^{56}Fe.

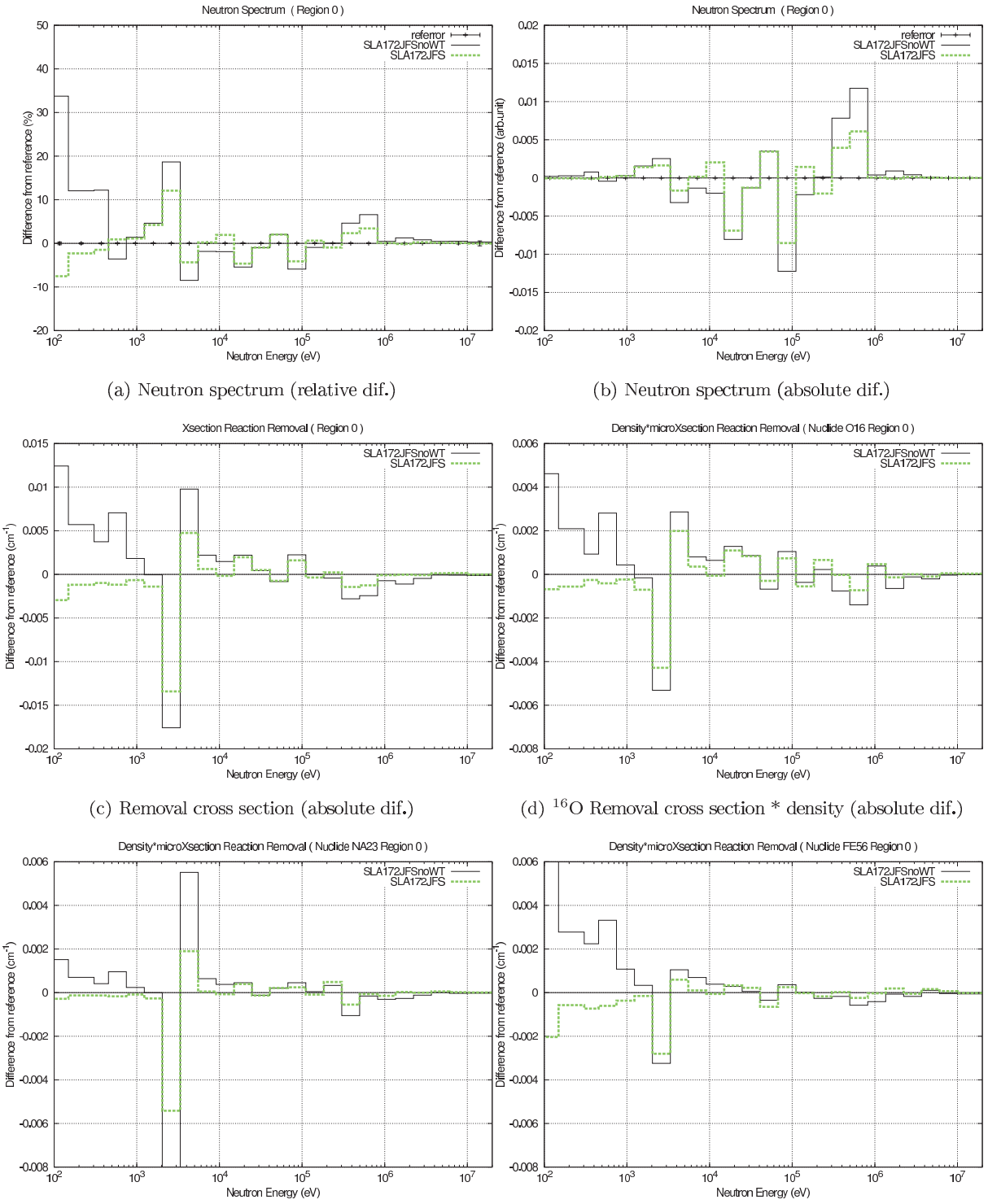

(a) Neutron spectrum (relative dif.)

(b) Neutron spectrum (absolute dif.)

(c) Removal cross section (absolute dif.)

(d) ^{16}O Removal cross section * density (absolute dif.)

(e) ^{23}Na Removal cross section * density (absolute dif.)

(f) ^{56}Fe Removal cross section * density (absolute dif.)

Fig. 5.4.5 Effect of weight function on neutron spectrum and removal cross section (SLA1968 as reference)

5.4.3 Effect of background cross section iteration

In the present work, an iteration procedure for background cross sections was not employed to make comparisons simple. An effect of the iteration is investigated by comparing SLA172JFSnoR with the iteration procedure (named "SLA172JFSnoRIte") and SLA172JFS in the homogeneous cell model. If the iteration procedure is effective, resonance overlap effects between ^{239}Pu and ^{238}U are considered to some extent and SLA172JFSnoRIte results should be closer to SLA172JFS results than SLA172JFSnoR results.

Figure 5.4.6 compares cross sections for nuclides of interest. We can see that the iteration procedure is effective in general. In particular, large improvement is found in ^{239}Pu capture cross sections below several 100 eV.

An exception is in the ^{238}U capture and scattering cross sections around 3 keV. The values deviate from SLA172JFS when the iteration procedure is applied. However, in this case, the deviation from SLA172JFS has no meaning since the resonance overlap effect is dominant between ^{23}Na and ^{238}U. The accuracy of the capture cross section becomes worse by the iteration, whereas that of the scattering cross section becomes better. This contradiction indicates that the problem would be in the infinite cross section, that is, weight function used is not good enough.

Figure 5.4.7 shows the iteration effect on the reaction rates. The effect is so small that we can see the discussions made so far are not affected by the use of iteration procedure.

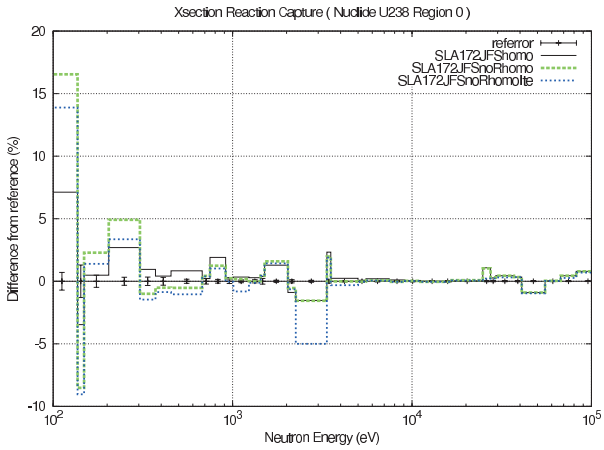

(a) ^{238}U capture

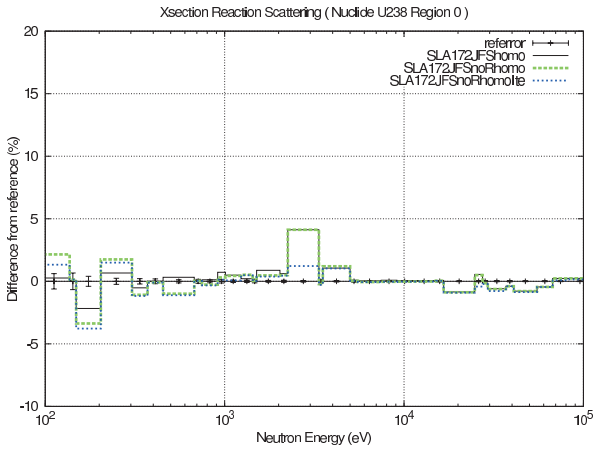

(b) ^{238}U scattering

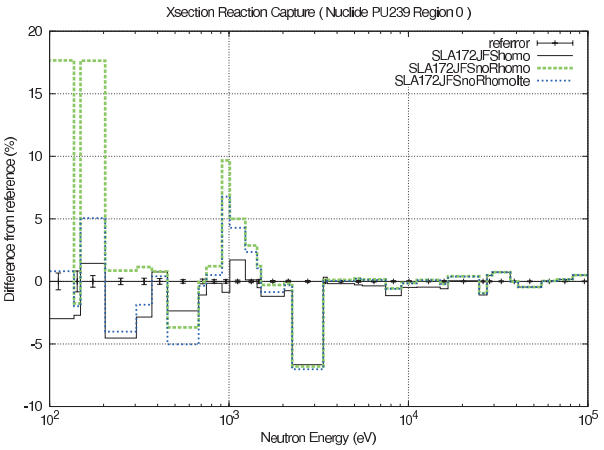

(c) ^{239}Pu capture

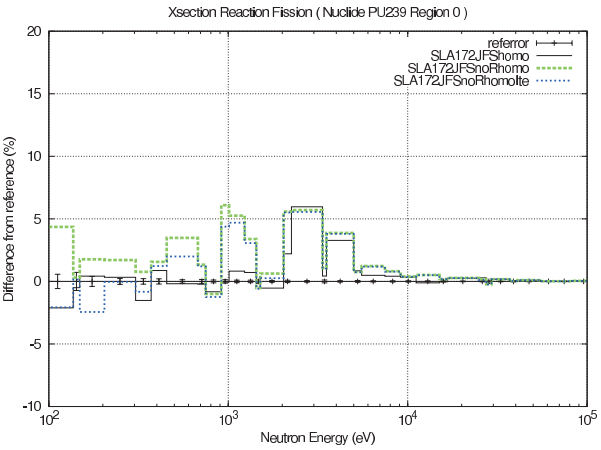

(d) ^{239}Pu fission

Fig. 5.4.6 Effect of iteration on cross sections (standard level homo cal.)

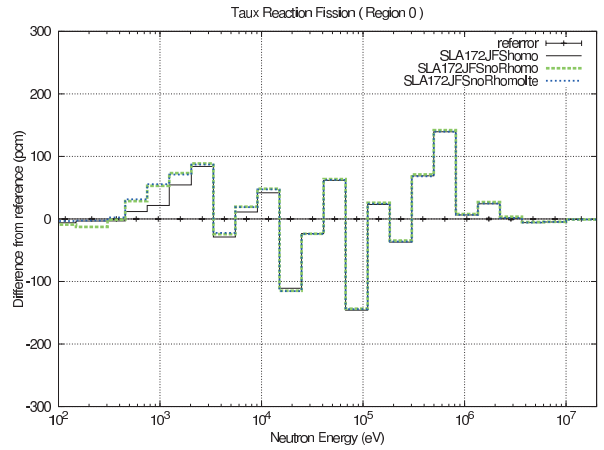

(a) Fission reaction rate (absolute dif.)

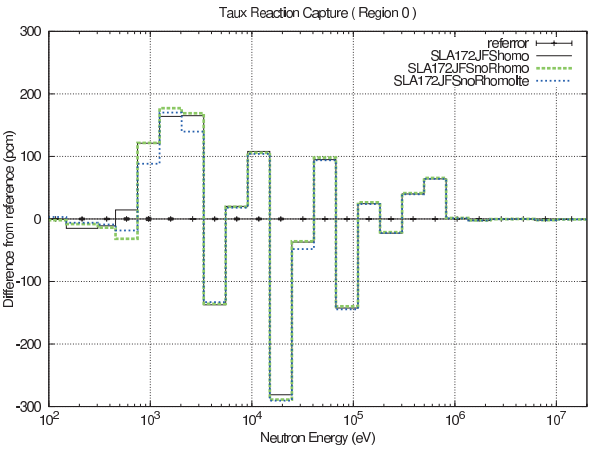

(b) Capture reaction rate (absolute dif.)

Fig. 5.4.7 Effect of iteration on reaction rates (stand rd level homo cal.)

6. Conclusions

A lattice cell benchmark calculation was carried out for APOLLO2 and SLAROM-UF on the infinite lattice of a simple pin cell featuring a fast reactor.

The accuracy was compared on k-infinity and reaction rates in the two kinds of reference level calculations and in the standard level calculations. All the calculations were performed with JEFF-3.1.

In the 1st reference level calculation, APOLLO2 and SLAROM-UF agreed with the reference value of k-infinity obtained by a continuous energy Monte Carlo calculation within 50pcm. However, larger errors were observed in cross sections in a particular energy range. The problems are

- ^{239}Pu cross sections in the unresolved energy range in both codes,
- incident energy of χ spectrum in APOLLO2,
- ^{23}Na cross sections around 50 keV in APOLLO2 reference level calculation,
- ^{56}Fe cross sections around 40 keV in SLAROM-UF reference level calculation.

The former three problems are on the cross section library. The 1st one for APOLLO2 and the 3rd one appear only in the sub-group calculation, and the library creation code CALENDF may need modification. The last one is associated with a restriction of the ultra-fine group calculation.

In the 2nd reference level calculation, which is based on the ECCO 1968 group structure, both results agreed with the reference value of k-infinity within 100pcm. In comparison with the 1st reference level calculation, the resonance overlap effect was observed by several percents in cross sections of heavy nuclides.

In the standard level calculation based on the APOLLO2 library creation methodology, a discrepancy appeared by more than 300pcm.

A restriction has been found in applying APOLLO2 to a fast reactor analysis. The APOLLO2 172 group library does not have a sufficiently small background cross section to evaluate the self-shielding effect on ^{56}Fe cross sections. The mixture self-shielding treatment recently introduced in APOLLO2 was tentatively applied and found effective to solve the problem.

SLAROM-UF standard calculation uses a larger approximation in treating a heterogeneous cell. The error was observed by several percents in ^{238}U capture cross section.

SLAROM-UF original standard level calculation based on its library creation methodology is the best among the standard level calculations. Improvement from the SLAROM-UF standard level calculation is achieved mainly by use of a proper weight function for light or intermediate nuclides.

Acknowledgments

The authors wish to thank all the people in CEA who provided us with useful and helpful assistance. Particular thanks are given to Mireille COSTE-DELCLAUX for preparing codes and data essential to this work as well as technical advice over all the work, to Pierre BELLIER for his technical support in using APOLLO2 and TRIPOLI, to Claude MOUNIER for giving us input data to create cross section libraries, to Stephane MENGELLE for instruction on the reference level calculation, and to Jean-Michel DO for technical support in understanding APOLLO2.

References

1) S. Loubiere, R. Sanchez, M.Coste, et al.,"APOLLO2 Twelve Years Later", Mathematics and Computation, Reactor Physics and Environmental Analysis in Nuclear Applications, Madrid, vol. 2, p.1298-1315, Madrid, Spain (1999).

2) R.E.MacFarlane, NJOY99.0: code system for producing pointwise and multigroup neutron and photon cross sections from ENDF/B data, Los Alamos National Laboratory, Los Alamos, NM (1999).

3) J-Ch. Sublet, P. Ribon, and M. Coste, CALENDF computer code, CEA/DEN Cadarache Report No. CEA-R-6020, (2003).

4) T.Hazama, G.Chiba, and K.Sugino, "Development of a Fine and Ultra-Fine Group Cell Calculation Code SLAROM-UF for Fast Reactor Analyses," J. Nucl. Sci. Technol., 43[8], p.908 (2006).

5) S.Katsuragi, T.Tone, and A.Hasegawa: JAERI Fast Reactor Group Constants Systems Part I, JAERI 1195 (1970).

6) D.E.CULLEN, PREPRO 2004: 2004 ENDF/B Pre-processing codes IAEA-NDS-39, Rev. 12, (2004).

7) H.Takano, Y. Ishiguro, and Y. Matsui, TIMS-1:A Processing Code for Production of Group Constants of Heavy Resonant Nuclei, JAERI 1267 (1980).

8) P.H.Kier and A.A.Robba, RABBLE: A Program for Computation of Resonance Absorption in Multiregion Reactor Cells, ANL-7326 (1967).

9) T.Tone, "A Numerical Study of Heterogeneity Effects in Fast Reactor Critical Assemblies," J. Nucl. Sci. Technol., 12[8], p.467 (1975).

10) G.Rimpault: Physics Documentation of ERANOS: The ECCO Cell Code, RT-SPRC-LEPh-97-001 (1997).

11) J. P. Both, A. Mazzolo, O. Petit, Y. Peneliau, and B. Roesslinger, User Manual for version 4.3 of the TRIPOLI-4 Monte Carlo method particle transport computer code, CEA-Report : CEA-R-6044, DTI, CEA/Saclay, France, (2003).

12) Y. Nagaya, K. Okumura, T. Mori, and M. Nakagawa: MVP/GMVP II : General Purpose Monte Carlo Codes for Neutron and Photon Transport Calculations based on Continuous Energy and Multigroup Methods JAERI-1348 (2005).

13) A.Koning, R.Forrest, M.Kellett, R.Mills, H.Henriksson, and Y.Rugama: "The JEFF-3.1 Nuclear Data Library," JEFF Report 21 (2006).

14) M. Coste and S. Mengelle: "New Resonant Mixture Self-Shielding Treatment in the Code APOLLO2", PHYSOR 2004, 95586.pdf, Chicago, (2004).

Appendix A Comparison of Self-Shielding Factors

The self-shielding (SS) factors are compared among calculations with different cell models and energy group structures. The factors were obtained from SLAROM-UF calculations performed in a slightly modified cell model in which a set of nuclides with a very small density (1×10^{-10}barn-cm) were added to the original cell model as a different nuclide so that the self-shielding effects on the added nuclide were treated independently. Thus obtained cross sections of the added nuclides are of the infinite dilution. Then the SS factor were obtained by the ratio of the original cross sections to the added.

Figures A.1 to A.3 compare the SS factors for major nuclides and reactions among SLA172, SLA172homo, and SLA1968homo.

The difference between the cell models (SLA172 and SLA172homo) do not exceed a few percents. The heterogeneous effect on the SS factor is not large in the present cell model.

In the 172 group calculations, the SS factors on the removal cross sections are significantly different from those on the scattering cross section, whereas they are similar in the 1968 group calculation.

This is the reason that the self-shielding effect on scattering matrix should be considered by the TRSS option in the AP172 calculation.

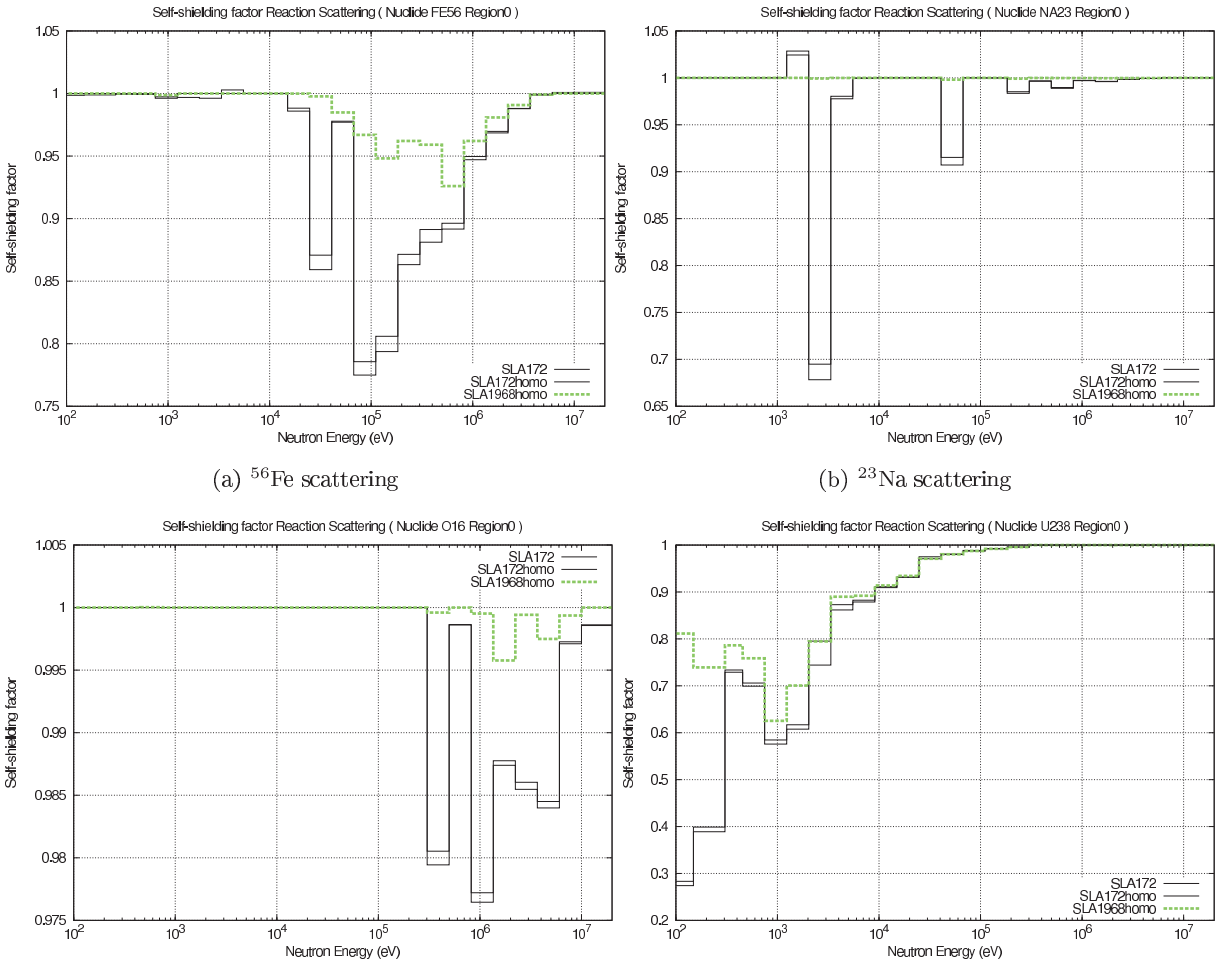

(a) ^{56}Fe scattering

(b) ^{23}Na scattering

(c) ^{16}O scattering

(d) ^{238}U scattering

Fig. A.1 Comparison of self-shielding factors (scattering)

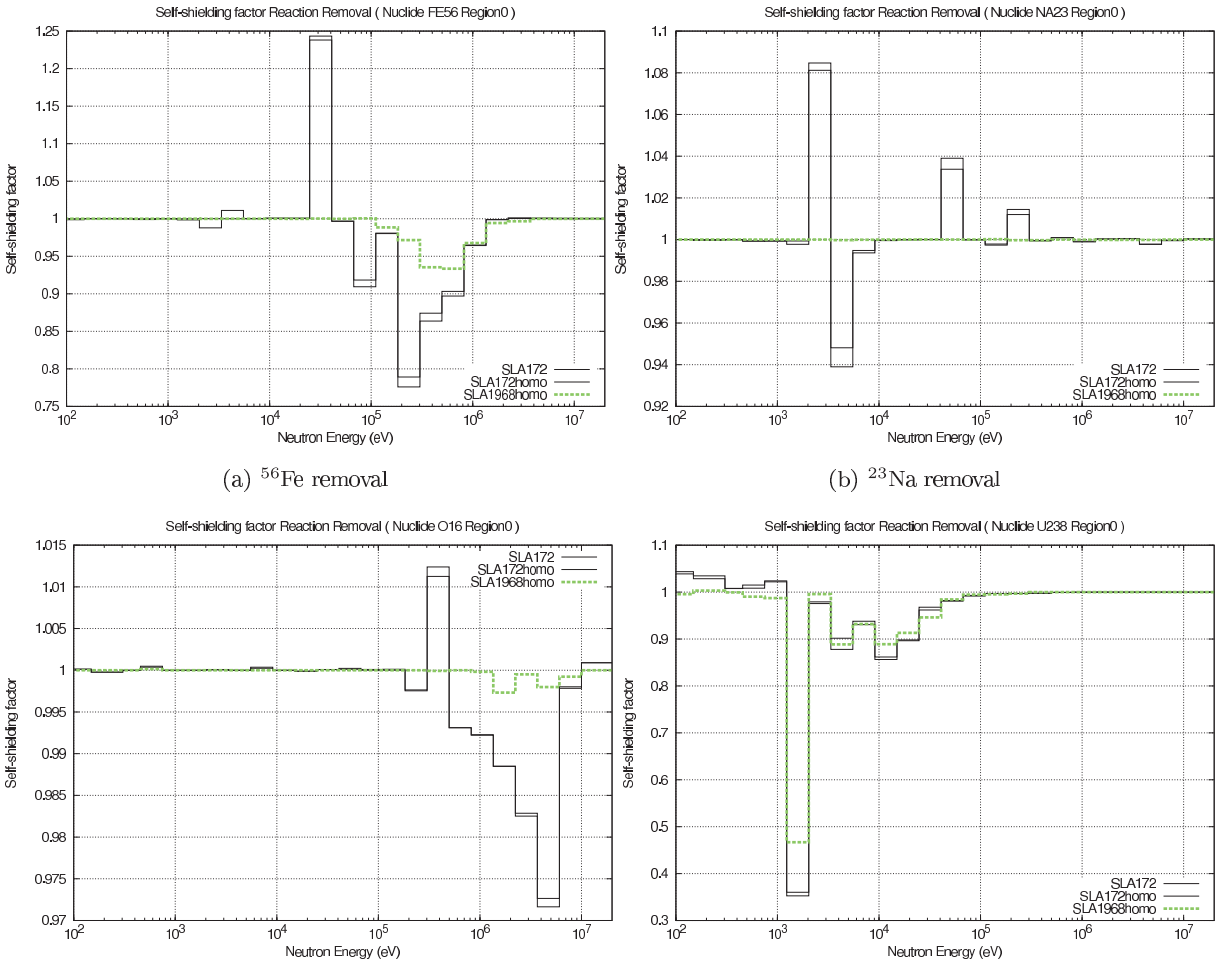

(a) ^{56}Fe removal

(b) ^{23}Na removal

(c) ^{16}O removal

(d) ^{238}U removal

Fig. A.2 Comparison of self-shielding factors (removal, including inelastic scattering)

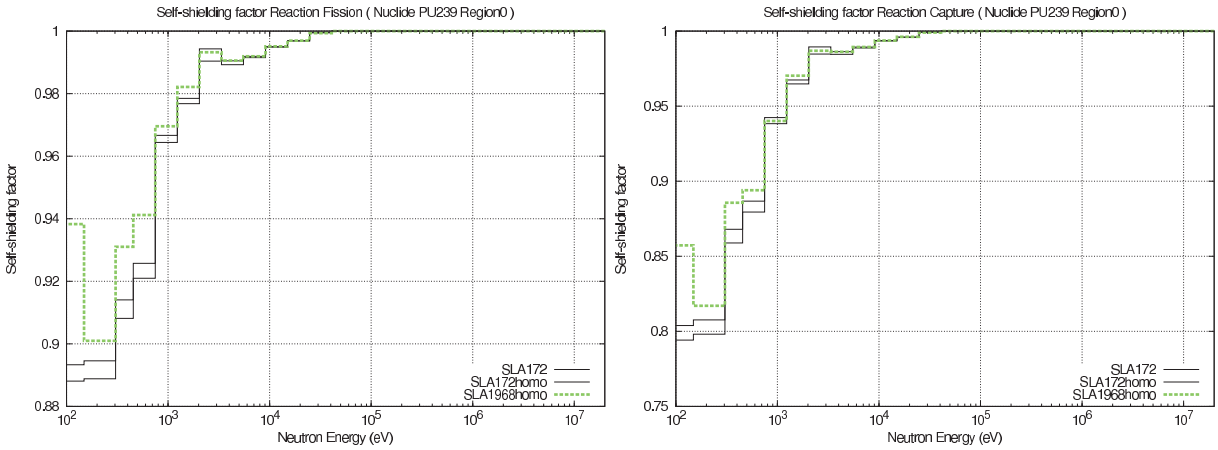

(a) ^{239}Pu fission

(b) ^{239}Pu capture

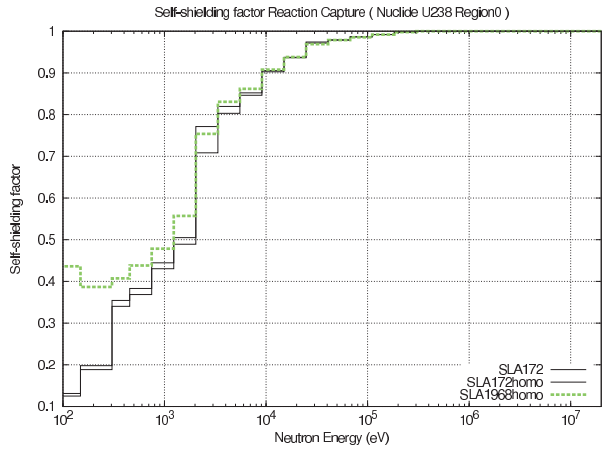

(c) ^{238}U capture

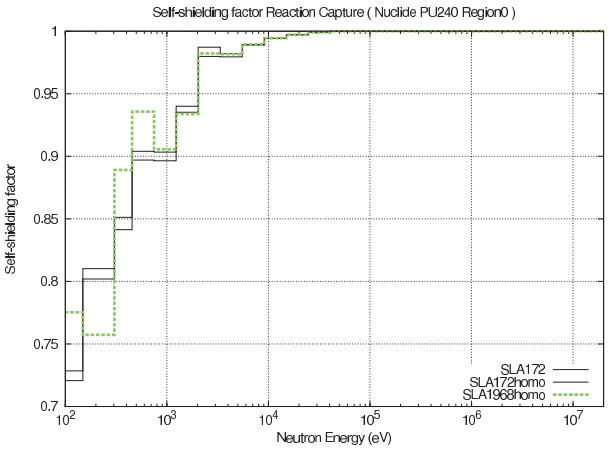

(d) ^{240}Pu capture

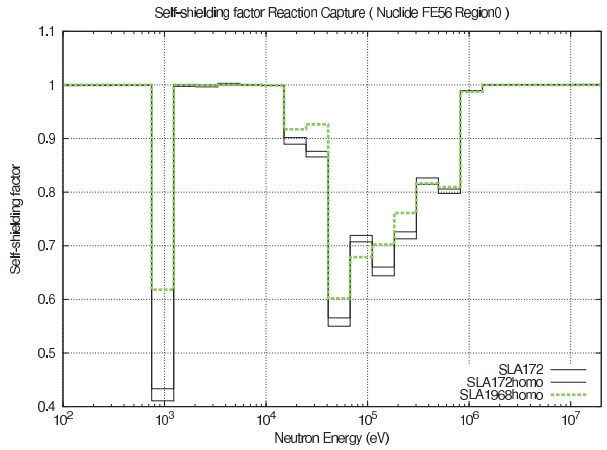

(e) ^{56}Fe capture

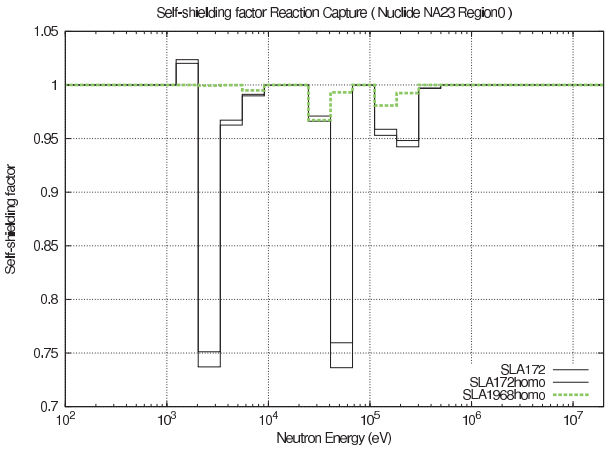

(f) ^{23}Na capture

Fig. A.3 Comparison of self-shielding factors (fission and capture)

This is a blank page.

国際単位系（SI）

表１．SI 基本単位

基本量	SI 基本単位	
	名称	記号
長さ	メートル	m
質量	キログラム	kg
時間	秒	s
電流	アンペア	A
熱力学温度	ケルビン	K
物質量	モル	mol
光度	カンデラ	cd

表２．基本単位を用いて表されるSI組立単位の例

組立量	SI 基本単位	
	名称	記号
面積	平方メートル	m^2
体積	立法メートル	m^3
速さ，速度	メートル毎秒	m/s
加速度	メートル毎秒毎秒	m/s^2
波数	毎メートル	m^{-1}
密度，質量密度	キログラム毎立方メートル	kg/m^3
面積密度	キログラム毎平方メートル	kg/m^2
比体積	立方メートル毎キログラム	m^3/kg
電流密度	アンペア毎平方メートル	A/m^2
磁界の強さ	アンペア毎メートル	A/m
量濃度[(a)]，濃度	モル毎立方メートル	mol/m^3
質量濃度	キログラム毎立法メートル	kg/m^3
輝度	カンデラ毎平方メートル	cd/m^2
屈折率[(b)]	（数字の） 1	1
比透磁率[(b)]	（数字の） 1	1

(a) 量濃度（amount concentration）は臨床化学の分野では物質濃度（substance concentration）ともよばれる。
(b) これらは無次元量あるいは次元１をもつ量であるが、そのことを表す単位記号である数字の１は通常は表記しない。

表３．固有の名称と記号で表されるSI組立単位

組立量	SI 組立単位			
	名称	記号	他のSI単位による表し方	SI基本単位による表し方
平面角	ラジアン[(b)]	rad	1[(b)]	m/m
立体角	ステラジアン[(b)]	sr[(c)]	1[(b)]	m^2/m^2
周波数	ヘルツ[(d)]	Hz		s^{-1}
力	ニュートン	N		m kg s^{-2}
圧力，応力	パスカル	Pa	N/m^2	m^{-1} kg s^{-2}
エネルギー，仕事，熱量	ジュール	J	N m	m^2 kg s^{-2}
仕事率，工率，放射束	ワット	W	J/s	m^2 kg s^{-3}
電荷，電気量	クーロン	C		s A
電位差（電圧），起電力	ボルト	V	W/A	m^2 kg s^{-3} A^{-1}
静電容量	ファラド	F	C/V	m^{-2} kg^{-1} s^4 A^2
電気抵抗	オーム	Ω	V/A	m^2 kg s^{-3} A^{-2}
コンダクタンス	ジーメンス	S	A/V	m^{-2} kg^{-1} s^3 A^2
磁束	ウエーバ	Wb	Vs	m^2 kg s^{-2} A^{-1}
磁束密度	テスラ	T	Wb/m^2	kg s^{-2} A^{-1}
インダクタンス	ヘンリー	H	Wb/A	m^2 kg s^{-2} A^{-2}
セルシウス温度	セルシウス度[(e)]	℃		K
光束	ルーメン	lm	cd sr[(c)]	cd
照度	ルクス	lx	lm/m^2	m^{-2} cd
放射性核種の放射能[(f)]	ベクレル[(d)]	Bq		s^{-1}
吸収線量，比エネルギー分与，カーマ	グレイ	Gy	J/kg	m^2 s^{-2}
線量当量，周辺線量当量，方向性線量当量，個人線量当量	シーベルト[(g)]	Sv	J/kg	m^2 s^{-2}
酸素活性	カタール	kat		s^{-1} mol

(a)SI接頭語は固有の名称と記号を持つ組立単位と組み合わせても使用できる。しかし接頭語を付した単位はもはやコヒーレントではない。
(b)ラジアンとステラジアンは数字の１に対する単位の特別な名称で、量についての情報をつたえるために使われる。実際には、使用する時には記号rad及びsrが用いられるが、習慣として組立単位としての記号である数字の１は明示されない。
(c)測光学ではステラジアンという名称と記号srを単位の表し方の中に、そのまま維持している。
(d)ヘルツは周期現象についてのみ、ベクレルは放射性核種の統計的過程についてのみ使用される。
(e)セルシウス度はケルビンの特別な名称で、セルシウス温度を表すために使用される。セルシウス度とケルビンの単位の大きさは同一である。したがって、温度差や温度間隔を表す数値はどちらの単位で表しても同じである。
(f)放射性核種の放射能（activity referred to a radionuclide）は、しばしば誤った用語で"radioactivity"と記される。
(g)単位シーベルト（PV,2002,70,205）についてはCIPM勧告2（CI-2002）を参照。

表４．単位の中に固有の名称と記号を含むSI組立単位の例

組立量	SI 組立単位		
	名称	記号	SI 基本単位による表し方
粘度	パスカル秒	Pa s	m^{-1} kg s^{-1}
力のモーメント	ニュートンメートル	N m	m^2 kg s^{-2}
表面張力	ニュートン毎メートル	N/m	kg s^{-2}
角速度	ラジアン毎秒	rad/s	m m^{-1} s^{-1}=s^{-1}
角加速度	ラジアン毎秒毎秒	rad/s^2	m m^{-1} s^{-2}=s^{-2}
熱流密度，放射照度	ワット毎平方メートル	W/m^2	kg s^{-3}
熱容量，エントロピー	ジュール毎ケルビン	J/K	m^2 kg s^{-2} K^{-1}
比熱容量，比エントロピー	ジュール毎キログラム毎ケルビン	J/(kg K)	m^2 s^{-2} K^{-1}
比エネルギー	ジュール毎キログラム	J/kg	m^2 s^{-2}
熱伝導率	ワット毎メートル毎ケルビン	W/(m K)	m kg s^{-3} K^{-1}
体積エネルギー	ジュール毎立方メートル	J/m^3	m^{-1} kg s^{-2}
電界の強さ	ボルト毎メートル	V/m	m kg s^{-3} A^{-1}
電荷密度	クーロン毎立方メートル	C/m^3	m^{-3} sA
表面電荷	クーロン毎平方メートル	C/m^2	m^{-2} sA
電束密度，電気変位	クーロン毎平方メートル	C/m^2	m^{-2} sA
誘電率	ファラド毎メートル	F/m	m^{-3} kg^{-1} s^4 A^2
透磁率	ヘンリー毎メートル	H/m	m kg s^{-2} A^{-2}
モルエネルギー	ジュール毎モル	J/mol	m^2 kg s^{-2} mol^{-1}
モルエントロピー，モル熱容量	ジュール毎モル毎ケルビン	J/(mol K)	m^2 kg s^{-2} K^{-1} mol^{-1}
照射線量（X線及びγ線）	クーロン毎キログラム	C/kg	kg^{-1} sA
吸収線量率	グレイ毎秒	Gy/s	m^2 s^{-3}
放射強度	ワット毎ステラジアン	W/sr	m^4 m^{-2} kg s^{-3}=m^2 kg s^{-3}
放射輝度	ワット毎平方メートル毎ステラジアン	W/(m^2 sr)	m^2 m^{-2} kg s^{-3}=kg s^{-3}
酵素活性濃度	カタール毎立方メートル	kat/m^3	m^{-3} s^{-1} mol

表５．SI 接頭語

乗数	接頭語	記号	乗数	接頭語	記号
10^{24}	ヨタ	Y	10^{-1}	デシ	d
10^{21}	ゼタ	Z	10^{-2}	センチ	c
10^{18}	エクサ	E	10^{-3}	ミリ	m
10^{15}	ペタ	P	10^{-6}	マイクロ	μ
10^{12}	テラ	T	10^{-9}	ナノ	n
10^{9}	ギガ	G	10^{-12}	ピコ	p
10^{6}	メガ	M	10^{-15}	フェムト	f
10^{3}	キロ	k	10^{-18}	アト	a
10^{2}	ヘクト	h	10^{-21}	ゼプト	z
10^{1}	デカ	da	10^{-24}	ヨクト	y

表６．SIに属さないが、SIと併用される単位

名称	記号	SI 単位による値
分	min	1 min=60s
時	h	1h =60 min=3600 s
日	d	1 d=24 h=86 400 s
度	°	1°=(π/180) rad
分	’	1’=(1/60)°=(π/10800) rad
秒	”	1”=(1/60)’=(π/648000) rad
ヘクタール	ha	$1ha=1hm^2=10^4m^2$
リットル	L，l	$1L=11=1dm^3=10^3cm^3=10^{-3}m^3$
トン	t	$1t=10^3$ kg

表７．SIに属さないが、SIと併用される単位で、SI単位で表される数値が実験的に得られるもの

名称	記号	SI 単位で表される数値
電子ボルト	eV	$1eV=1.602\ 176\ 53(14)\times10^{-19}J$
ダルトン	Da	$1Da=1.660\ 538\ 86(28)\times10^{-27}kg$
統一原子質量単位	u	1u=1 Da
天文単位	ua	$1ua=1.495\ 978\ 706\ 91(6)\times10^{11}m$

表８．SIに属さないが、SIと併用されるその他の単位

名称	記号	SI 単位で表される数値
バール	bar	1 bar=0.1MPa=100kPa=10^5Pa
水銀柱ミリメートル	mmHg	1mmHg=133.322Pa
オングストローム	Å	1 Å=0.1nm=100pm=10^{-10}m
海里	M	1 M=1852m
バーン	b	$1\ b=100fm^2=(10^{-12}cm)2=10^{-28}m^2$
ノット	kn	1 kn=(1852/3600)m/s
ネーパ	Np	SI単位との数値的な関係は、対数量の定義に依存。
ベル	B	
デジベル	dB	

表９．固有の名称をもつCGS組立単位

名称	記号	SI 単位で表される数値
エルグ	erg	$1\ erg=10^{-7}$ J
ダイン	dyn	$1\ dyn=10^{-5}$N
ポアズ	P	$1\ P=1\ dyn\ s\ cm^{-2}=0.1Pa\ s$
ストークス	St	$1\ St=1cm^2\ s^{-1}=10^{-4}m^2\ s^{-1}$
スチルブ	sb	$1\ sb=1cd\ cm^{-2}=10^4cd\ m^{-2}$
フォト	ph	$1\ ph=1cd\ sr\ cm^{-2}\ 10^4lx$
ガル	Gal	$1\ Gal=1cm\ s^{-2}=10^{-2}ms^{-2}$
マクスウェル	Mx	$1\ Mx = 1G\ cm^2=10^{-8}Wb$
ガウス	G	$1\ G=1Mx\ cm^{-2}=10^{-4}T$
エルステッド[(c)]	Oe	1 Oe ≙ $(10^3/4\pi)A\ m^{-1}$

(c) ３元系のCGS単位系とSIでは直接比較できないため、等号「 ≙ 」は対応関係を示すものである。

表10．SIに属さないその他の単位の例

名称	記号	SI 単位で表される数値
キュリー	Ci	$1\ Ci=3.7\times10^{10}Bq$
レントゲン	R	$1\ R=2.58\times10^{-4}C/kg$
ラド	rad	$1\ rad=1cGy=10^{-2}Gy$
レム	rem	$1\ rem=1\ cSv=10^{-2}Sv$
ガンマ	γ	1γ=1 nT=10-9T
フェルミ		1フェルミ=1 fm=10-15m
メートル系カラット		1メートル系カラット = 200 mg = 2×10-4kg
トル	Torr	1 Torr = (101 325/760) Pa
標準大気圧	atm	1 atm = 101 325 Pa
カロリー	cal	1cal=4.1858J（「15℃」カロリー），4.1868J（「IT」カロリー）4.184J（「熱化学」カロリー）
ミクロン	μ	1 μ =1μm=10^{-6}m

（第8版，2006年改訂）

この印刷物は再生紙を使用しています